

DRAFT DISCLAIMER

This contractor document was prepared for the U.S. Department of Energy (DOE), but has not undergone programmatic, policy, or publication review, and is provided for information only. The document provides preliminary information that may change based on new information or analysis, and is not intended for publication or wide distribution; it is a lower level contractor document that may or may not directly contribute to a published DOE report. Although this document has undergone technical reviews at the contractor organization, it has not undergone a DOE policy review. Therefore, the views and opinions of authors expressed do not necessarily state or reflect those of the DOE. However, in the interest of the rapid transfer of information, we are providing this document for your information, per your request.

DFO3
011

OFFICE OF CIVILIAN RADIOACTIVE WASTE MANAGEMENT
ANALYSIS/MODEL REVISION RECORD
Complete Only Applicable Items

1. Page: 2 of: 48

2. Analysis or Model Title:
Water Diversion Model

3. Document Identifier (including Rev. No. and Change No., if applicable):
ANL-EBS-MD-000028 REV 00

4. Revision/Change No.

5. Description of Revision/Change

00A	Issued for Checking
00B	Issued for Review
00C	Issued for Final check
00	Initial Issue

OFFICE OF CIVILIAN RADIOACTIVE WASTE MANAGEMENT
ANALYSIS/MODEL REVISION RECORD
Complete Only Applicable Items

1. Page: 2 of: 48

2. Analysis or Model Title:
Water Diversion Model

3. Document Identifier (including Rev. No. and Change No., if applicable):
ANL-EBS-MD-000028 REV 00

4. Revision/Change No.

5. Description of Revision/Change

00A	Issued for Checking
00B	Issued for Review
00C	Issued for Final check
00	Initial Issue

CONTENTS

	Page
1. PURPOSE.....	6
2. QUALITY ASSURANCE.....	7
3. COMPUTER SOFTWARE AND MODEL USAGE.....	7
4. INPUTS.....	8
4.1 DATA AND PARAMETERS	8
4.1.1 Drip Shield Construction	8
4.1.2 Select Liquid Properties of Water.....	8
4.1.3 Overton Sand Backfill Grain Density	9
4.1.4 Crushed Tuff Invert Grain Density and Specific Heat.....	9
4.1.5 Hydrologic and Geotechnical Properties of Overton Sand and Crushed Tuff.....	9
4.1.6 Drip Shield Geometry for the Flow Exclusion Analysis and the Bounding Calculation.....	9
4.2 CRITERIA	9
4.2.1 Drip Shield Material	9
4.2.2 Ex-Container System	9
4.2.3 Backfill.....	10
4.3 CODES AND STANDARDS.....	10
5. ASSUMPTIONS.....	10
5.1 INVERT MATERIAL	10
5.2 BACKFILL MATERIAL	10
5.3 EXCLUSION OF THE EVAPORATION AT THE DRIP SHIELD	10
5.4 CAPILLARY TUBES OF CREVICES HAVE THE SAME LENGTH.....	10
5.5 WATER FLOW BOUNDARIES ARE COMPOSED ENTIRELY OF SOLID- WATER BOUNDARIES.....	11
5.6 THEORETICAL APERTURE DIMENSION CREATED BY OVERLAPPING DRIP SHIELDS.....	11
5.7 THEORETICAL TREATMENT OF THE OVERLAP	11
5.8 WETTING ANGLE SET TO ZERO	11
5.9 MOISTURE RETENTION OF THE COMBINED MATERIAL.....	11
5.10 SATURATED HYDRAULIC CONDUCTIVITY OF THE COMBINED MATERIAL.....	12
5.11 FLOW ENTERING THE DRIFT ENTERS IMMEDIATELY ABOVE THE WASTE PACKAGES.....	12
5.12 NEGLIGIBLE CORROSION OF THE DRIP SHIELD	12
5.13 MAXIMUM PERCOLATION RATE AT THE REPOSITORY HORIZON.....	12
5.14 STEADY STATE FLOW.....	12
6. ANALYSIS/MODEL	12
6.1 DEVELOPMENT OF A CONCEPTUAL MODEL FOR THE DRIP SHIELD PERFORMANCE AND DIVERSION.....	12

6.2	HYDROLOGIC AND THERMAL PROPERTIES OF ENGINEERED BARRIER COMPONENTS	15
6.2.1	Properties of the Backfill	16
6.2.2	Properties of the Invert Material	22
6.2.3	Properties of the Altered Invert.....	26
6.2.4	Hydrological Properties of the Drip Shield	28
6.2.5	Bounding Calculation for the Drip Shield	37
6.3	CONCEPTUAL FLOW DIVERSION MODEL BASED UPON CLOSED-FORM ANALYTICAL SOLUTIONS	39
7.	CONCLUSIONS.....	42
8.	REFERENCES	45
8.1	DOCUMENTS CITED.....	45
8.2	CODES, STANDARDS, REGULATIONS, AND PROCEDURES.....	47
8.3	SOURCE DATA.....	48
9.	ATTACHMENTS.....	48
ATTACHMENT I	THIS SECTION IS RESERVED.....	I-1
ATTACHMENT II	ACRONYMS AND ABBREVIATIONS	II-1
ATTACHMENT III	LIST OF SYMBOLS	III-1
ATTACHMENT IV	MOISTURE RETENTION CHARACTERISTICS OF THE BACKFILL AND INVERT MATERIALS.....	IV-1
ATTACHMENT V	FLOW EXCLUSION ANALYSIS.....	V-1
ATTACHMENT VI	BOUNDING ANALYSIS FOR A DRIP SHIELD	VI-1

FIGURES

		Page
1	Conceptual Model for Diversion of Water Flow	13
2	Technical Approach for Evaluating Flow through the Backfill and Drip Shield	14
3	Grain Size Distribution for Overton Sand	17
4	Moisture Retention Relationship for Backfill Material	19
5	Relationship of Volumetric Moisture Content to Unsaturated Hydraulic Conductivity for Backfill	20
6	Unsaturated Hydraulic Conductivity versus Moisture Potential for Backfill	22
7	Moisture Retention Relationship for the Invert	24
8	Unsaturated Hydraulic Conductivity versus Volumetric Moisture Content for the Invert	25
9	Unsaturated Hydraulic Conductivity versus Moisture Potential for the Invert	26
10	Moisture Retention Relationship for the Combined Material	27
11	Unsaturated Hydraulic Conductivity versus Moisture Potential for a Combined Material	28
12	Concept for Distribution of Capillary Tube Bundles at Some Time	30
13	Relationship of Moisture Potential to Relative Humidity	33
14	Relationship of Hydraulic Conductivity to Moisture Potential Using the Exponential Relationship	35
15	Seepage About Cylindrical Drip Shield	37
16	Bounding Relationship of the Equivalent Conductivity for the Drip Shield to Moisture Potential	39
17	Conceptual Network Resistance Model for the Water Diversion Model	42

1. PURPOSE

The distribution of seepage in the proposed repository will be highly variable due in part to variations in the spatial distribution of percolations. The performance of the drip shield and the backfill system may divert the water flux around the waste packages to the invert. Diversion will occur along the drift surface, within the backfill, at the drip shield, and at the Waste Package (WP) surface, even after the drip shield and WP have been breached by corrosion.

The purpose and objective of this Analysis and Modeling Report (AMR) are to develop a conceptual model and constitutive properties for bounding the volume and rate of seepage water that flows around the drip shield (CRWMS M&O 1999c). This analysis model is to be compatible with the selected repository conceptual design (Wilkins and Heath, 1999) and will be used to evaluate the performance of the Engineered Barrier System (EBS), and to provide input to the EBS Water Distribution and Removal Model. This model supports the Engineered Barrier System (EBS) postclosure performance assessment for the Site Recommendation (SR).

This document characterizes the hydrological constitutive properties of the backfill and invert materials (Section 6.2) and a third material that represents a mixture of the two. These include the Overton Sand which is selected as a backfill (Section 5.2), crushed tuff which is selected as the invert (Section 5.1), and a combined material (Sections 5.9 and 5.10) which has retention and hydraulic conductivity properties intermediate to the selected materials for the backfill and the invert. The properties include the grain size distribution, the dry bulk density and porosity, the moisture retention, the intrinsic permeability, the relative permeability, and the material thermal properties. The van Genuchten relationships with curve fit parameters are used to define the basic retention relationship of moisture potential (Ψ) to volumetric moisture content (Θ), and the basic relationship of unsaturated hydraulic conductivity to volumetric moisture content (Θ). The van Genuchten curve fit parameters were determined from a least squares fit to the measured Unsaturated Flow Apparatus (UFA) data for Overton Sand backfill and the crushed tuff invert. These constitutive properties are direct inputs to the Non-isothermal Unsaturated saturated Flow and Transport (NUFT) codes and characterize the constitutive properties for these materials within the Engineered Barrier System (EBS).

Models are currently being developed for pitting and general corrosion of the drip shield. This AMR develops flow analysis methods (Section 6.2.4) to bound the diversion performance of the drip shield at different stages of degradation by corrosion. Further, this report also develops flow analysis methods for the conceptual model under the assumption of negligible corrosion of the drip shield (Section 5.12) as indicated by design studies (TBV-3808). The conceptual model can be used to bound the diversion performance of the drip shield. In addition, this report provides a simple bounding calculation for assessing flow through apertures within the drip shield (Section 5.4 to 5.8). The bounding calculation uses several assumptions (Sections 5.4 to 5.8). The flow relationship presented in Section 6.2.5 can be used in conjunction with a NUFT analysis of moisture potential around the DS to bound the flow through the drip shield. As an alternative to performing NUFT calculations to assess the partitioning of flow, an analysis approach based upon a closed-form analytical solution at isothermal temperature is developed in Section 6.3.

2. QUALITY ASSURANCE

In accordance with QAP-2-0 *Conduct of Activities*, it has been determined (CRWMS M&O 1999b) that this document is subject to the quality assurance controls of the *Quality Assurance Requirements and Description* (QARD) (U.S. DOE 1998a). The design analysis *Classification of the MGR Ex-Container System* (CRWMS M&O 1999a), performed in accordance with QAP-2-3 *Classification of Permanent Items*, has concluded that the drip shield is Quality Level 1 (QL-1). The development plan for this document, *Development Plan for the Water Diversion Model* (CRWMS M&O 1999c), was prepared in accordance with AP-2.13Q, *Technical Product Development Planning*. The Water Diversion Model document is prepared in accordance with AP-3.10Q, *Analyses and Models*. Unqualified inputs will be identified and tracked in accordance with AP-3.15Q, *Managing Technical Product Inputs*.

3. COMPUTER SOFTWARE AND MODEL USAGE

The RETC (REtention and Conductivity fitting) Version 1.1 (Software Tracking Number (STN) 10099-1.1-00) computer program was used for curvefitting to estimate the saturated hydraulic conductivity for the invert (0.60 cm/sec) as contained in Section 6.2.2.4 and on page IV-14 in Attachment IV. The results of the van Genuchten parameters from the RETC program corroborate the estimated van Genuchten parameters from the EXCEL calculations. The program may be used to fit several analytical models to observed water retention and/or unsaturated hydraulic conductivity data (van Genuchten et al. 1991, p. 2). The software is currently unqualified and the output is assigned TBV-3924. However, the process for software qualification has been initiated under AP-SI.1Q *Software Management*.

The computer programs *Microsoft Excel 97* and *Mathcad 8 Professional* (MathSoft 1998) were used in the preparation of this model. These software items are appropriate for this application. These software items were used to perform support calculations and are not a controlled source of information. Thus, they are not subject to software management per AP-SI.1Q. However, software routines are controlled in accordance with AP-SI.1Q and are documented where used.

Microsoft Excel 97 is a commercial spreadsheet program designed to assist in routine calculations. The program is used in Attachment IV to perform curvefitting to the van Genuchten retention relationship. The Solver is an add-in function in EXCEL. The Solver can minimize a target cell that involves multiple cell variables that might be subject to multiple constraints. The Solver is used specifically to solve for several variables under the constraint for a target value. In this case it is the minimization of the least squares of the volumetric moisture content for curvefitting. Also, the program provides other built-in mathematical functions that can be used together with user-defined formulas for the van Genuchten relations discussed subsequently in Section 6.2 to automate the calculation process. Output formulas are automatically updated as input data are added or changed. *Microsoft Excel 97* also includes a graphics package to assist in plotting the curvefits against the data presented in Attachment IV.

Mathcad 8 is an all-purpose program that has many built-in functions for performing and documenting mathematical calculations. *Mathcad 8* was used for linear regression analysis and water exclusion analysis, and to plot functions in Attachments V and VI. The following provides

a brief discussion of the application of MathCad 8 in this AMR. The user defined functions used in MathCad are verified by hand calculations.

Attachment IV presents calculations for moisture retention characteristics of the backfill and the invert. These calculations involve inputting vectors of tabulated data; using vector and matrix operations to combine the data; defining functions for moisture retention and unsaturated hydraulic conductivity as discussed subsequently; plotting the results of curvefitting against data; performing linear regression analysis using MathCad functions for linear regression analysis, and using user defined functions for determining the retention relationship for the combined material

Attachment V presents calculations for a flow exclusion analysis. In this analysis, a function, defined by the user, is presented for calculating a dimensionless ratio as discussed subsequently in Section 6.2.4.2. The function defined by the user, applies built in Mathcad Bessel functions to generate a contour plot of the dimensionless ratio I.

Attachment VI presents a bounding analysis for a drip shield using Mathcad 8. In this attachment, the properties of liquid water are input to a function defined in Section 6.2.5. A second user defined function is presented for the backfill. An x-y plot is developed showing the relationship of the backfill conductivity to the bounding curve for the drip shield.

4. INPUTS

4.1 DATA AND PARAMETERS

4.1.1 Drip Shield Construction

The drip shield (illustrated in Figure 1) is constructed of titanium, grade 7 (Wilkins and Heath 1999, Encl. 2, Requirements 9.0, p. 2). The drip shield is 2 centimeters thick and has an inside radius of 1.231 meters (DTN: SN9908T0872799.004) (TBV-3471).

4.1.2 Select Liquid Properties of Water

The select properties of water at 60° C are listed below (Lide and Frederikse 1997, p. 6-3). This temperature is selected for modeling purposes because it is representative of the post closure environment. It is being used in the EBS Pilot Scale Test #3 as described in *Planning Guidance for EBS Test Number 3 – Drip Shield Test* (CRWMS M&O 1999f, p. 3).

Surface Tension (σ) mN/m	Dynamic Viscosity (ν) $\mu\text{Pa} \cdot \text{s}$	Density (ρ_w) g/cm^3
66.24	466.5	0.98320

4.1.3 Overton Sand Backfill Grain Density

The grain density of the backfill is 2.7 g/cm^3 (DTN: SN9908T0872799.004) (TBV-3471).

4.1.4 Crushed Tuff Invert Grain Density and Specific Heat

The grain density of the invert material is 2.53 g/cm^3 , and the specific heat value is 948 J/Kg-K (DTN: SN9908T0872799.004) (TBV-3471).

4.1.5 Hydrologic and Geotechnical Properties of Overton Sand and Crushed Tuff

The hydrologic and geotechnical properties for the crushed tuff for two samples sieved between 2.0 and 4.75 mm are taken from U. S. Geological Survey (USGS) testing entitled *Water Retention and Unsaturated Hydraulic Conductivity Measurements for Various Size Fractions of Crushed, Sieved, Welded Tuff Samples Measured Using a Centrifuge* (DTN: GS980808312242.015) (TBV - 3799). These data sets are illustrated in Figures 7 and 8.

The hydrologic and geotechnical properties for the Overton Sand are taken from *Particle Size Data, Water Retention Data, and Hydraulic Conductivity Data for Overton Sand Used In The Water Diversion Model AMR (ANL-EBS-MD-000028 Rev 00)* (DTN: MO9912EBSPWR28.001) for two samples sieved between 0.1 and 1.0 mm (TBV-3518). These data sets are illustrated in Figures 4 and 5.

Note further that other properties such as van Genuchten curve fit parameters and thermal properties are developed further in Sections 6.2.1 to 6.2.3.

4.1.6 Drip Shield Geometry for the Flow Exclusion Analysis and the Bounding Calculation

The drip shield length is 5.485 meters. The drip shield overlap dimension is 10 cm. This is used in the Bounding Analysis for a Drip Shield in Attachment VI. These values are taken from the *Drip Shield Design* transmittal (CRWMS M&O 1999d, Item 2) (TBV-3796).

4.2 CRITERIA

4.2.1 Drip Shield Material

The "Direction to Transition to Enhanced Design Alternative II" letter, Enclosure 2 –Guidelines for Implementation of EDA II (Wilkins and Heath 1999, Enclosure 2, Requirements 9.0, p. 2), specifies that the drip shield will be titanium grade 7, at least 2 centimeters thick. From this statement it is inferred that a drip shield will be part of the Ex-Container design.

4.2.2 Ex-Container System

The *Ex-Container System Description Document* (CRWMS M&O 1998, p. 4 of 19) states that "the Ex-Container System consists of the waste package support hardware (pedestal and pier) and any performance enhancing barriers (i.e., sorptive inverts, backfill, and drip shields) installed or placed in the emplacement drift". It is implicit that the drip shield is considered a part of the

Ex-container System. Further, Section 1.1.1, states "the system contributes to the isolation of waste from the Natural Barrier." and Section 1.1.3 states "the system minimizes the amount of water contacting the waste package ...". From these sections it is inferred that a drip shield is part of the Ex-Container System and it is necessary to be included in modeling.

4.2.3 Backfill

The "Direction to Transition to Enhanced Design Alternative II" letter, Enclosure 2-Guidelines for Implementation of EDA II (Wilkins and Heath 1999, Enclosure 2, Requirements 7.0, p. 2), specifies that the design will include backfill.

4.3 CODES AND STANDARDS

Not used.

5. ASSUMPTIONS

5.1 INVERT MATERIAL

The invert material is crushed tuff from the Tptpl lithostratigraphic unit which is part of the TSw2 thermal/mechanical unit (CRWMS M&O 1997, p. 23) (TBV - 3797). The Repository Host Horizon is located mainly in the TSw2 unit. The invert material hydrological properties are presently unavailable for the Tptpl formation. Properties for the Tptpmn are used in this analysis in place of Tptpl values because they are both part of the TSw2 thermal/mechanical unit (CRWMS M&O 1997, p. 23). After crushing tuff, it is not expected that the matrix properties of the tuff aggregate would be different between these subunits. This assumption is used throughout. This assumption requires laboratory testing for confirmation (TBV-3810).

5.2 BACKFILL MATERIAL

The backfill material is assumed to be Overton Sand. The "Direction to Transition to Enhanced Design Alternative II" letter (Wilkins and Heath 1999, Encl. 2, Requirements 7.0, p. 2) says that quartz sand is a candidate backfill material. This assumption is used throughout. This assumption requires laboratory testing for confirmation (TBV-3811).

5.3 EXCLUSION OF THE EVAPORATION AT THE DRIP SHIELD

In this model, water is assumed not to evaporate. Normally, water that flows to the drip shield would evaporate and this evaporation at the drip shield surface would reduce the potential flow rate. Therefore it is conservative to exclude evaporation for purposes of calculating the flow rate through the drip shield at isothermal temperatures. This assumption is used through out as a bounding condition.

5.4 CAPILLARY TUBES OF CREVICES HAVE THE SAME LENGTH

All capillary tubes or crevices (due to pitting or crevice corrosion) in the model are assumed to have the same length, which is equal to the thickness of the drip shield (Δt). The basis for this

assumption is that soil structures are frequently modeled in this manner (Jury et al. 1991, p. 90) and it is reasonable to expect that the drip shield thickness would be uniform. Further, this assumption provides a bounding analysis in that the shortest path length through the drip shield is selected. This assumption is used in Section 6.2.4 (TBV-3800).

5.5 WATER FLOW BOUNDARIES ARE COMPOSED ENTIRELY OF SOLID-WATER BOUNDARIES

The water flow boundaries are composed entirely of solid-water boundaries. The basis for this assumption is that water would not flow through empty void spaces and would completely wet other void spaces (Jury et al. 1991, p. 90). This assumption is used throughout. This assumption requires laboratory testing for confirmation (TBV-3801).

5.6 THEORETICAL APERTURE DIMENSION CREATED BY OVERLAPPING DRIP SHIELDS

The flow through the interface of the drip shield overlap, at a specific moisture potential, is a function of the moisture retention and flow characteristics of the aperture. For the purposes of a bounding calculation, the thickness of the aperture, at the specified moisture potential, is assumed to be equal to the maximum aperture thickness that could retain water in the aperture. The basis for this assumption is that it is conservative to assume that water flow is governed by the maximum aperture thickness, since the presence of narrower apertures would result in lower flow rates through the aperture under the same moisture gradient. This assumption is used in Sections 6.2 and 6.2.5 (TBV-3803).

5.7 THEORETICAL TREATMENT OF THE OVERLAP

The overlap of the drip shield is described as a parallel plate in the model. Hence the capillary rise law for parallel plates (Kwicklis and Healy 1993, p. 4094) can be applied. The basis for this assumption is the flow of water, through capillary tubes or plates, is opposed by viscous forces according to Newton's law of viscosity (Jury et al. 1991, p.42). This assumption is used in Section 6.2.5. This assumption requires laboratory testing for confirmation (TBV-3802).

5.8 WETTING ANGLE SET TO ZERO

The wetting angle between the drip shield surface and the liquid water is assumed to be equal to zero (CRWMS M&O 1999e, p. 1, Response 6). The basis for this assumption is that it is conservative to set the wetting angle to zero. This assumption does not require confirmation since it is a bounding assumption. This assumption is used in Section 6.2.4 (TBV-3804).

5.9 MOISTURE RETENTION OF THE COMBINED MATERIAL

It is assumed that the moisture content relationship for the reference backfill and the invert can be weighted equally. The basis for this assumption is that Campbell (1985, p. 46) presents a relationship for mixtures of materials and it is reasonable to assume equal weighting. This assumption requires confirmation through laboratory and field testing to determine the moisture retention of the combined material. This assumption is used in Section 6.2.3 (TBV-3805).

5.10 SATURATED HYDRAULIC CONDUCTIVITY OF THE COMBINED MATERIAL

The saturated hydraulic conductivity of the combined material is equal to the harmonic mean for the backfill and invert materials. The basis for this assumption is that the finer texture of the finer material would likely govern the resistance to flow. This assumption requires confirmation through laboratory testing to determine the saturated hydraulic conductivity (TBV-3806).

5.11 FLOW ENTERING THE DRIFT ENTERS IMMEDIATELY ABOVE THE WASTE PACKAGES

The flow entering the drift from seepage is assumed to enter immediately above the waste package. The basis for this assumption is that for a closed-form analytical model, the assumption is conservative since flow that enters to the side of the WP would be imbibed by the surrounding fractured media. This assumption is bounding and does not require confirmation. This assumption is used throughout (TBV-3807).

5.12 NEGLIGIBLE CORROSION OF THE DRIP SHIELD

The analysis assumes negligible corrosion of the drip shield due to localized and general corrosion. The basis for this assumption is that the drip shield is comprised of titanium, which is a highly corrosion resistant material. This assumption is used in Section 6.2.5. This assumption requires confirmation (TBV-3808).

5.13 MAXIMUM PERCOLATION RATE AT THE REPOSITORY HORIZON

To evaluate the performance of the backfill under extreme conditions, a bounding percolation value that will require confirmation is used within the footprint of the repository. The bounding percolation rate at the repository horizon is 25 mm/yr (DTN: MO9901YMP98017.001). This assumption is used in Section 6.2.4.2. This assumption requires confirmation (TBV-3312).

5.14 STEADY STATE FLOW

The analysis assumes steady state flow. The basis for this assumption is that the capacitance of the fine pores in the drip shield is small over long time periods, and that the amount of water entering backfill pores, capillary tubes, or crevices would equal the amount of water exiting such crevices. This assumption is used through out as a bounding condition (TBV-3809).

6. ANALYSIS/MODEL

6.1 DEVELOPMENT OF A CONCEPTUAL MODEL FOR THE DRIP SHIELD PERFORMANCE AND DIVERSION

The drip shield is designed to divert water flow to the invert (Figure 1). A conceptual model is developed for how water is partitioned in the drift. As water enters the drift and flows through the backfill, the water flow will be partitioned into (1) water flow through the drip shield that contacts the waste packages; (2) water flow that flows through the backfill directly to the invert; and (3) water flow that contacts the drip shield but does not flow through the drip shield.

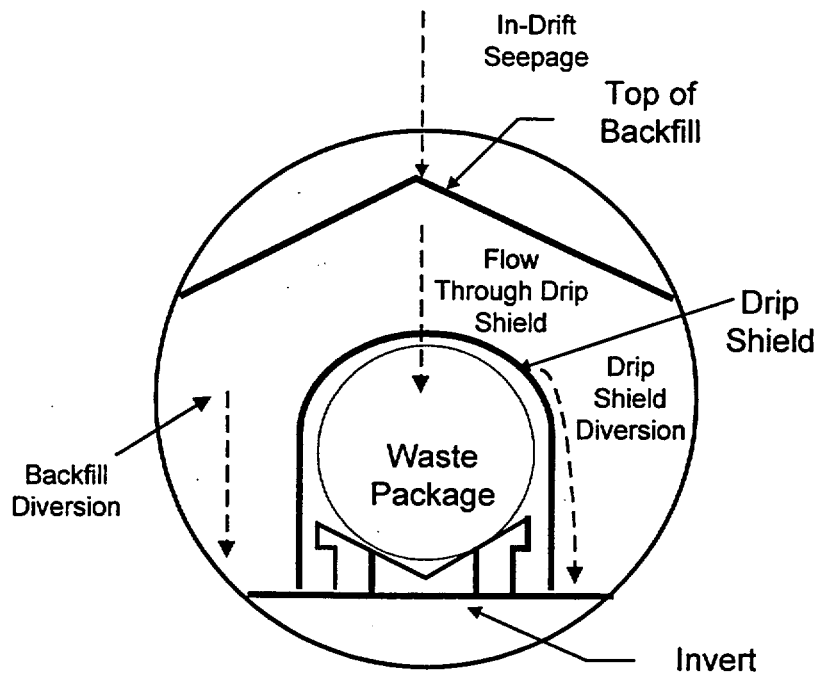


Figure 1. Conceptual Model for Diversion of Water Flow

The following section discusses how the water diversion and flow model is used to perform evaluations for flow through the drip shield. Figure 2 presents a flow chart for performing the assessment and identifies the relationship of the water diversion and flow model to other models and analyses. The shaded shapes show the water diversion and flow model that is discussed in detail. Note that model validation is not needed for a conceptual model.

Three principal analyses are significant to developing a model for flow through the drip shield. These include the physical/chemical environment of the drip shield, the Waste Package Degradation (WAPDEG) Model (DOE 1998b, Vol. 3, p. 3-77) to calculate the evolution of penetrations, and seepage flux calculations. The following presents a brief discussion of these analyses.

The conceptual model for drip shield degradation incorporates the important modes of corrosion. These corrosion modes include general corrosion, and localized corrosion. These corrosion processes are simulated through the model for degradation of corrosion resistant material and that may be modified for drip shield degradation. Also, the principal inputs include environmental factors such as temperature, relative humidity, mode of water contact, and chemical factors such as pH and concentration of aggressive species such as chloride, sulfate, nitrate, and carbonate, as well as metallurgical factors. Degradation modes for the candidate material for the drip shield may include general corrosion, pitting corrosion, stress corrosion cracking, galvanically enhanced corrosion, microbiologically influenced corrosion, radiation-induced corrosion, corrosion in welded materials, and high-temperature oxidation. The seepage flux model determines the amount of water entering the drift that could potentially contact the drip shield. The physical/chemical environment model determines the metallurgical and environmental factors affecting drip shield degradation.

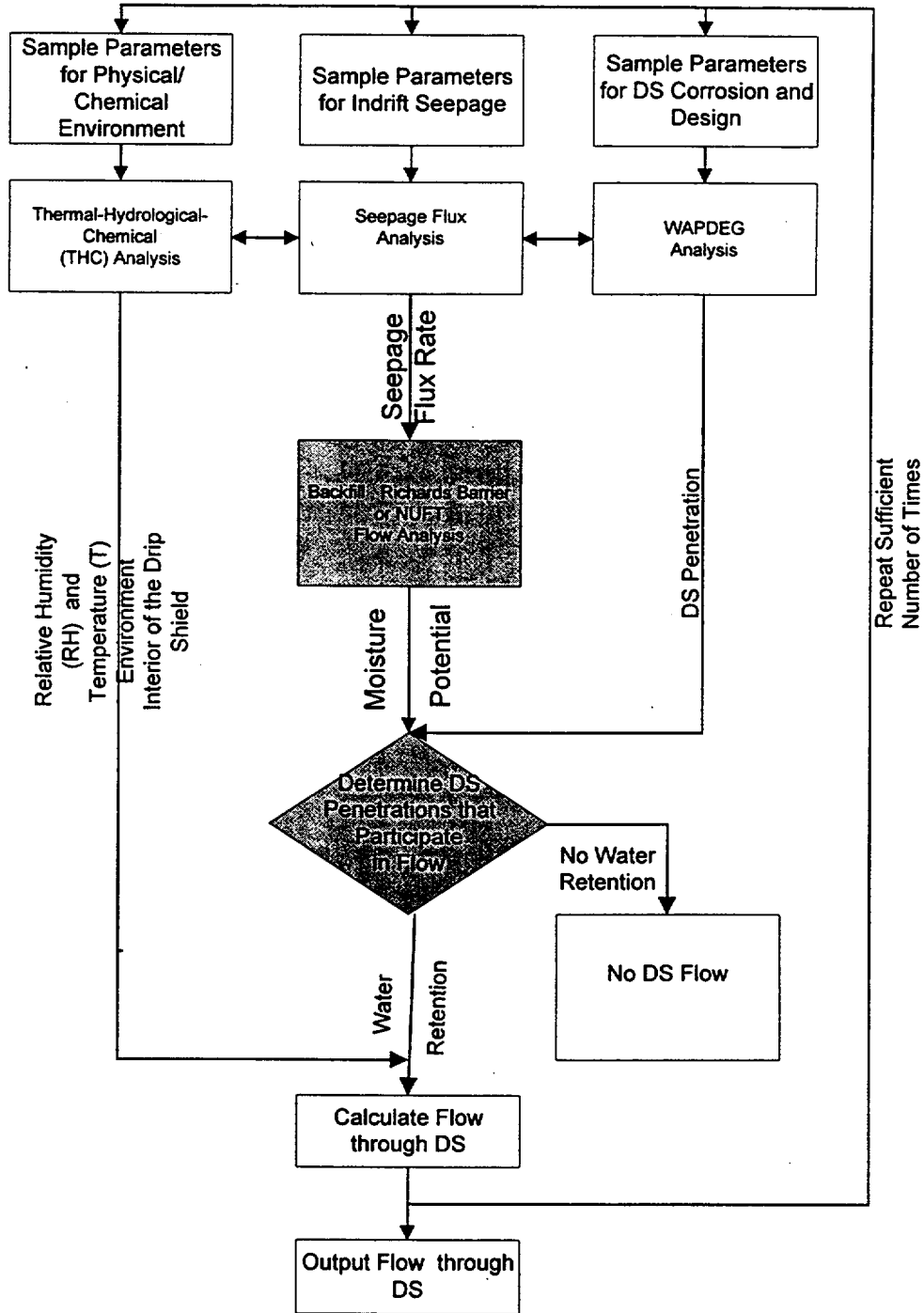


Figure 2. Technical Approach for Evaluating Flow through the Backfill and Drip Shield

The drip shield degradation model is currently under development. It is envisioned that Monte Carlo simulation methods (DOE 1998b, Vol. 3, p. 2-38) will be used to evaluate the evolution of drip shield degradation over time. In this analysis, a cumulative distribution function for seepage flux that is characterized by an expectation and variance or, alternately, by shape parameters, is sampled. The seepage flux distribution is determined by spatially variable host rock properties and variations in the ambient percolation flux at the repository horizon (DOE 1998b, Vol. 3, p. 2-18). In addition, the important parameters in the physical/chemical environment are sampled. This results in a single realization or set of parameters that is analyzed by deterministic methods in WAPDEG. The WAPDEG analysis is performed to determine the formation of pits and crevices on the drip shield and how they evolve with time for the single realization. By repeating this process many times, the distribution of outputs such as the pit and crevice corrosion distribution is obtained.

The capillary properties of the backfill and invert are significant in determining the moisture potential on the exterior of the drip shield. These properties include the relationship of hydraulic conductivity to moisture potential (ψ), and the relationship of volumetric moisture content (θ) to moisture potential (ψ), as well as thermal properties. Sections 6.2.1 and 6.2.2 discuss these properties in detail. Note that symbols used throughout the document are identified in Attachment III.

The current design as discussed in Section 6.2 involves the placement of a finer backfill over the coarser invert material. There is the potential for the backfill material to migrate into the invert material after emplacement. Section 6.2.3 presents an analysis of the retention characteristics for the combined material, and the estimated hydrologic properties.

Two categories of penetrations, presented in Section 6.2.4, represent circular pits and long penetrations. Section 6.2.4 develops the water retention relationship for the drip shield that can be determined by direct application of capillary tube or parallel plate theory. Knowledge of the distribution of penetrations, and their geometry allows determination of whether water is retained in the penetrations and whether they present a possible pathway for flow through the drip shield. As an alternate approach, a bounding calculation based upon the retention of water in the penetrations can be developed. By determining the moisture potential ψ_i on the inside of the drip shield, and by direct application of Poiseuille's Law, or Parallel Plate Theory (Section 6.2.4), the flow through the drip shield can be calculated.

The sources of uncertainty in the conceptual Water Diversion Model include the uncertainty in hydrologic properties for the backfill, the invert, and the drip shield; variability in drift seepage rates; and variability in corrosion properties. The Monte Carlo simulation discussed previously provides a means for accounting for the effects of uncertainty in flow rates.

6.2 HYDROLOGIC AND THERMAL PROPERTIES OF ENGINEERED BARRIER COMPONENTS

General guidance on the selection of materials was provided by Wilkins and Heath (Wilkins and Heath 1999, Enclosure 2, p. 2) on the basis of thermal, hydrological, and geochemical consequences. The guidance included selection of a ballast material for the invert, a backfill, and a drip shield.

Crushed tuff is selected for the invert (Section 5.1) to provide geochemical compatibility with the surrounding host rock. The basis for the selection of the crushed tuff is that the material provides diffusion-barrier performance when transport from the waste package to the rock wall is diffusion dominated. This could occur if a waste package is breached but the protecting drip shield is intact, so that the invert ballast material immediately below the drip shield is unsaturated and protected from advective flow from other engineered barrier components.

Overton sand is selected for the backfill material (Section 5.2). The basis for the selection of this fine sand is discussed subsequently in Sections 6.2.4 and 6.2.5. This material will work in conjunction with the nonporous drip shield comprised of titanium (Section 4.2.1) to divert water around the waste packages when a bounding assumption (Section 5.6) is made regarding the flow through apertures in the drip shield. The combination of a drip shield and backfill diverts flow in the same manner as a Richard's Barrier by providing a contrast in unsaturated hydraulic conductivity.

6.2.1 Properties of the Backfill

This section presents an analysis of the estimated flow properties for the Overton Sand that has been selected as the backfill in the reference design. The Overton Sand has been selected based upon its capillary retention characteristics as discussed in Section 6.2.4.

6.2.1.1 Grain Size Distribution

The Overton sand is described as a fine to medium sand. The grain size distribution curve for Overton Sand from sieve analysis is presented in Figure 3 (Section 4.1.5). The hydrological and thermal properties for this sand are presented below.

6.2.1.2 Dry Bulk Density and Porosity

The estimated solid density of the backfill material is 2.7 g/cm^3 (Section 4.1.3) corresponding to a bulk density of 1.59 g/cm^3 as calculated below. The emplaced porosity for the backfill is estimated to be 0.41. The porosity is taken as the average volumetric moisture content for the first and second Overton Sand samples near saturation from Tempe Cell or pressure cell tests (Section 4.1.5). Using the soil phase convention of setting the volume of the solids (V_s) equal to 1.0 cm^3 , the total volume (V_t) equals the volume of the voids (V_v) and the solids (V_s) (See Attachment III for a list of symbols):

$$V_t = V_v + V_s \quad (\text{Eq. 1})$$

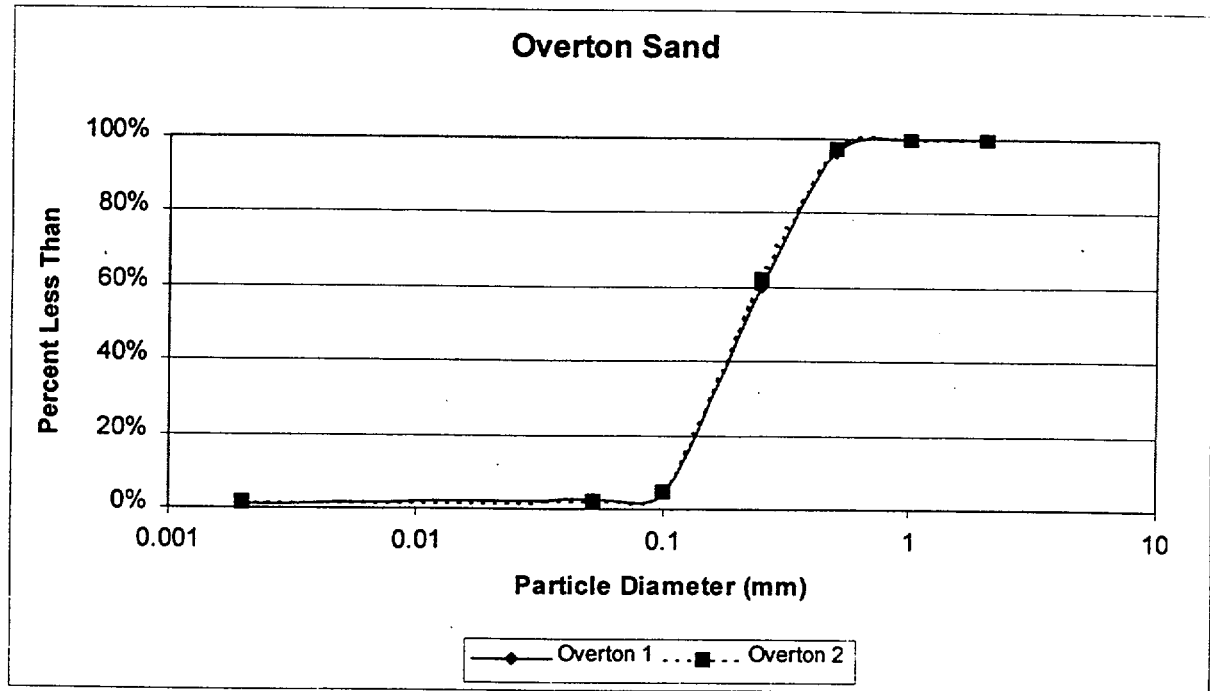


Figure 3. Grain Size Distribution for Overton Sand

The porosity (ϕ) is defined as the volume of the voids divided by the total volume:

$$\phi = V_v/V_t \quad (\text{Eq. 2})$$

$$V_v = 0.41V_t \quad (\text{Eq. 3})$$

Solving for V_v :

$$V_v = 0.41 (V_v+1.0)$$

$$V_v = 0.41/(1-0.41) = 0.695 \quad (\text{Eq. 4})$$

The dry bulk density (ρ) is defined as:

$$\rho = G_s V_s/V_t \quad (\text{Eq. 5})$$

The dry bulk density is calculated as:

$$\rho = 2.7 (1.0)/(0.695+1.0) = 1.59 \text{ g/cm}^3 \quad (\text{Eq. 6})$$

6.2.1.3 Moisture Retention

Moisture retention measurements were performed on the Overton Sand using two methods. These include the Unsaturated Flow Apparatus (UFA) measurements (CRWMS M&O 1996, Appendix C) and Tempe Cell or pressure cell measurements (Jury et al. 1991, p. 62).

The UFA mainly consists of an ultracentrifuge in which a soil sample is subject to centrifugal force. The volumetric moisture content (θ) as a function of the moisture potential (ψ) as discussed subsequently below can be determined by allowing the sample to drain until the moisture potential equals the centrifugal force per unit area divided by the unit weight in a state of equilibrium. The volumetric moisture content (θ) is determined gravimetrically using the bulk density of the sample.

The UFA represents an efficient method for testing fine-grained soils at higher moisture potential (ψ). For low moisture potentials, the Tempe Cell or pressure cell method was used (Jury et al. 1991, p. 62). The Tempe Cell consists of an airtight chamber with a freely draining, water saturated, porous ceramic plate on the bottom. The chamber is pressurized, which induces flow out of the sample through the porous cup. At equilibrium, flow through the tube is changed to zero and the moisture potential (ψ) can be calculated from the change in pressure. The volumetric moisture content is again determined gravimetrically.

Note that in the following discussion that moisture potential is a suction potential, and the convention is adopted for flow analysis in Section 6.2.4 that the moisture potential (ψ) is negative. The moisture retention and hydraulic conductivity relationships presented subsequently are functions of the absolute value of moisture potential (ψ).

The moisture retention data obtained from the two methods can be plotted and a curve fitting performed for the retention model based upon the van Genuchten two-parameter model $m=1-1/n$ (Fetter 1993, p. 172).

Define the moisture potential (capillary pressure divided by weight density) versus moisture content relation:

$$\theta(\alpha, n, \theta_s, \theta_r, \psi) = \left[1 + (|\psi\alpha|)^n \right]^{-m} (\theta_s - \theta_r) + \theta_r \quad (\text{Eq. 7})$$

For the two-parameter model, $m = 1-1/n$ (Fetter 1993, p. 172). Substituting this value of (m) into Equation (7) gives

$$\theta(\alpha, n, \theta_s, \theta_r, \psi) = \left[1 + (\psi\alpha)^n \right]^{-1 \left(1 - \frac{1}{n} \right)} (\theta_s - \theta_r) + \theta_r \quad (\text{Eq 8})$$

The van Genuchten curve-fitting parameters (θ_r , α_b , and n_b) were determined by fitting a curve to the retention data for the first Overton Sand sample using the *Microsoft Excel 97* equation solver (Attachment IV, p. IV-21). The saturated moisture content (θ_s) was determined from the Tempe Cell measurements as discussed above. The first Overton sand sample from the UFA measurements was used for curve fitting. For low volumetric moisture contents associated with high potential (greater than 360 cm) as discussed in Section 6.2.4, the first and second Overton Sand samples provided similar results. Also, the UFA measurements are more appropriate at the higher moisture potential. Figure 4 presents Equation (8) along with the UFA and Tempe Cell data for Overton sand.

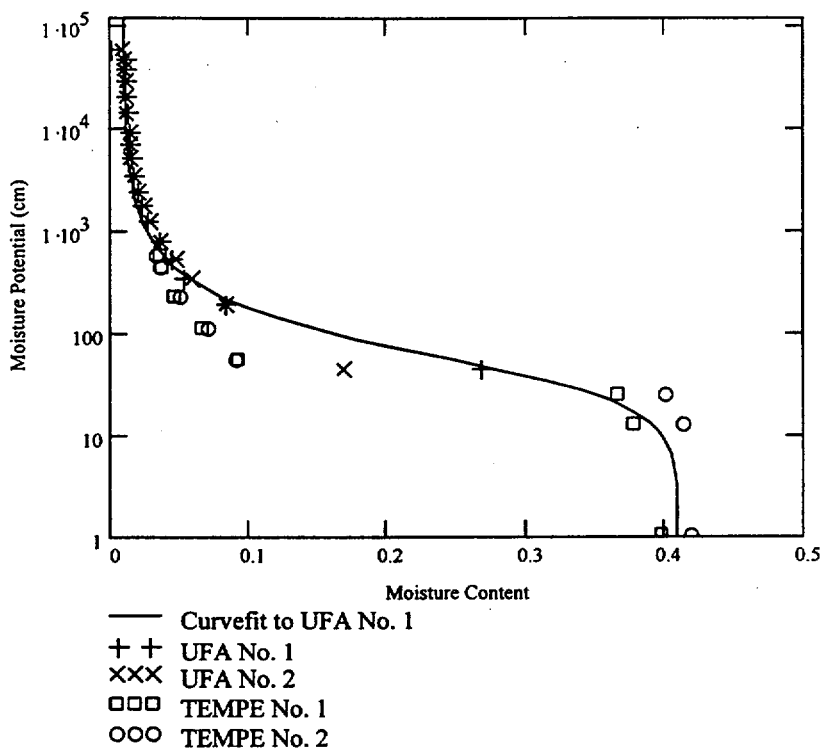


Figure 4. Moisture Retention Relationship for Backfill Material

A *Microsoft Excel 97* spreadsheet calculation using the *Microsoft Excel 97* Equation Solver is used to optimize the model parameters by fitting the closed-form mathematical expression in Equation (8) to the retention data. The estimated results from the curve-fitting process for the Overton Sand (Attachment IV, p. IV-21) are given below. Note that the units of measurement for moisture potential in the UFA testing are presented in units of bars as a suction pressure while the moisture potential for engineering analysis is in cm:

$$\theta_r = 0.01$$

$$\alpha_b = 0.03 \text{ (1/cm)}$$

$$n_b = 1.986$$

6.2.1.4 Intrinsic Permeability

The unsaturated flow properties data for sand were measured from UFA measurements as discussed subsequently. The saturated hydraulic conductivity of the backfill (K_s) is estimated to be 0.014 cm/sec by extrapolation of the unsaturated hydraulic conductivity versus volumetric moisture content θ relationship at a the value of the saturated volumetric moisture content (θ_s) or porosity(ϕ). The saturated hydraulic conductivity (Figure 5), corresponds to an approximate intrinsic permeability of $1.4 \times 10^{-7} \text{ cm}^2$.

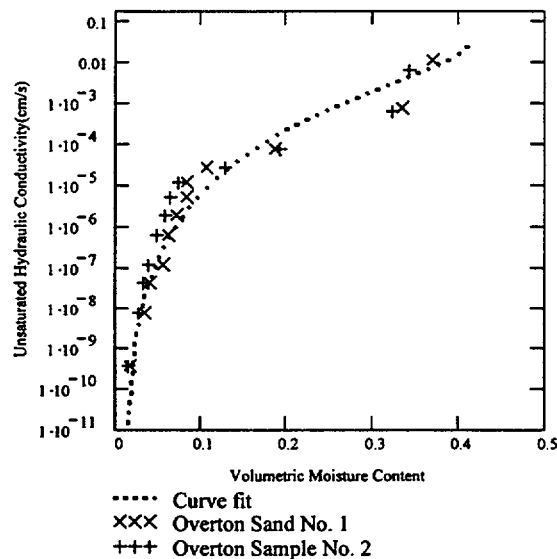


Figure 5. Relationship of Volumetric Moisture Content to Unsaturated Hydraulic Conductivity for Backfill

6.2.1.5 Relative Permeability

The UFA test apparatus described above is equipped with a constant ultra low flow pump that provides fluid to the sample through a rotating seal assembly and microdispersal system. This system can be used to determine the relationship between the unsaturated hydraulic conductivity (K_u) and volumetric moisture content through a direct application of Darcy's Law (CRWMS M&O 1996, Appendix C). Samples are spun at a constant rate to define the hydraulic gradient in the core. A constant flux is applied to the top of the core. The change in water content to carry the applied flux (flow rates to 0.001 ml/hr) at the applied gradient is measured. The unsaturated hydraulic conductivity can be determined from the ratio of the flow rate to the centrifugal force per unit volume (CRWMS M&O 1996, p. C-2).

The relationship of the unsaturated hydraulic conductivity with volumetric moisture content is given by (Jury et al. 1991, p. 109):

$$K(\theta) = K_s \left(\frac{\theta - \theta_r}{\theta_s - \theta_r} \right)^{\frac{1}{2}} \left[1 - \left[1 - \left(\frac{\theta - \theta_r}{\theta_s - \theta_r} \right)^{\frac{1}{1-\frac{1}{n}}} \right]^{\left(1-\frac{1}{n}\right)^2} \right] \quad (\text{Eq. 9})$$

This relationship is plotted against measured data for the first and second Overton Sand samples (Section 4.1.5) in Figure 5.

The wetting-phase relative permeability as a function of moisture potential for this model is restated from Fetter (1993, p. 182). The unsaturated hydraulic conductivity (wetting-phase relative permeability times saturated hydraulic conductivity) as a function of moisture potential is given below.

$$K(\alpha, n, \psi, K_s) = K_s \frac{\left[1 - (\alpha \psi)^{n-1} \left[1 + (\alpha \psi)^n \right]^{\left(-1+\frac{1}{n}\right)} \right]^2}{\left[1 + (\alpha \psi)^n \right]^{\left[\frac{1}{2} - \frac{1}{(2n)}\right]}} \quad (\text{Eq. 10})$$

The relative permeability function scales the saturated conductivity (K_s) to allow the unsaturated hydraulic conductivity function to be determined. Equation (10) with van Genuchten parameters (See Section 6.2.1.3) is used to plot the relationship for Overton Sand as shown in Figure 6.

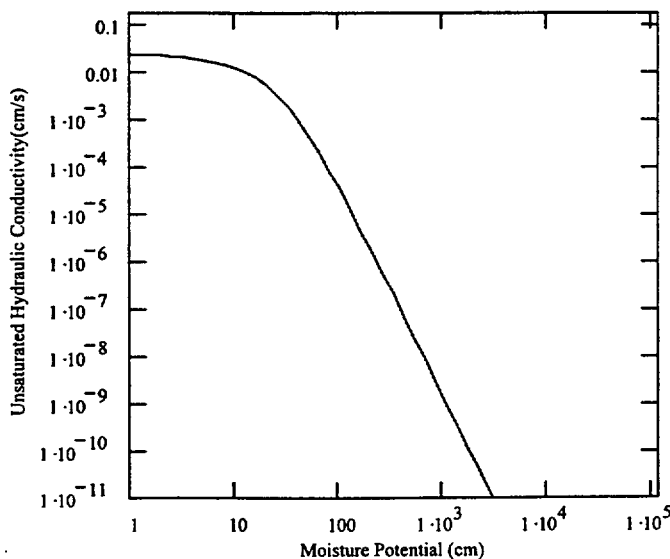


Figure 6. Unsaturated Hydraulic Conductivity versus Moisture Potential for Backfill

6.2.1.6 Material Thermal Properties

Thermal conductivity (K_s) is a strong function of water content (Jury et al. 1991, p. 183). For dry sand, the thermal conductivity at 20 °C is about 0.33 W/m³K (Lide and Frederikse 1997, p. 12 – 199). Jury et al. (1991, p. 179) presents a value for the specific heat (C_p) of a coarse quartz sand of 0.19 cal/(g °K). Converting the units from cal/g/°K to J/(kg °K) gives

$$C_p = 0.19 \frac{\text{cal}}{\text{g}^\circ\text{K}}$$

$$C_p = 795.42 \frac{\text{J}}{\text{kg}^\circ\text{K}}$$

The calculated value for C_p is 795.492 J/(kg°K) for the backfill. The thermal emissivity of the backfill is assumed to be equal to the emissivity for quartz on a rough surface, i.e., 0.93 (Holman 1997, p. 649).

6.2.2 Properties of the Invert Material

The invert material properties used in this model are described in the following sections.

6.2.2.1 Grain Size Distribution

The reference design includes crushed tuff. Crushed welded tuff sieved between 2.0 and 4.75 mm (Section 4.1.5) has been selected for pilot testing and the properties are described below for this material. The final design may require a different size distribution or material type, or both.

6.2.2.2 Bulk Density and Porosity

The reference invert fill material is assumed to be crushed tuff (Section 5.1). The U.S. Geological Survey measured the bulk density, water retention, and unsaturated hydraulic conductivity (Section 4.1.5). These were measured using the UFA. For materials sieved between 2.00 and 4.75 mm, used for hydraulic conductivity measurements (Section 4.1.5), the measured dry bulk density was 1.15 g/cm^3 as calculated below. The grain density is 2.53 g/cm^3 (Section 4.1.4). Calculate the porosity using the soil phase convention of setting the volume of the solids (V_s) equal to 1.0 cm^3 , developing a formula for the bulk density, and then calculating the volume of the voids. The dry bulk density is given by Equation (5) by noting that $V_t = V_s + V_v$:

$$\rho = G_s V_s / (V_s + V_v) \quad (\text{Eq. 11})$$

Substituting in the values for G_s , ρ , and V_s :

$$1.15 \text{ cm}^3 = 2.53 \text{ g/cm}^3 (1.0 \text{ cm}^3) / (1.0 \text{ cm}^3 + V_v) \quad (\text{Eq. 12})$$

Solve for V_v :

$$V_v = (2.53/1.15 - 1.0) \text{ cm}^3 \quad (\text{Eq. 13})$$

$$V_v = 1.209 \text{ cm}^3 \quad (\text{Eq. 14})$$

Solve for the porosity (ϕ)

$$\phi = 1.209 / (1.0 + 1.209) = 0.55 \quad (\text{Eq. 15})$$

6.2.2.3 Moisture Retention

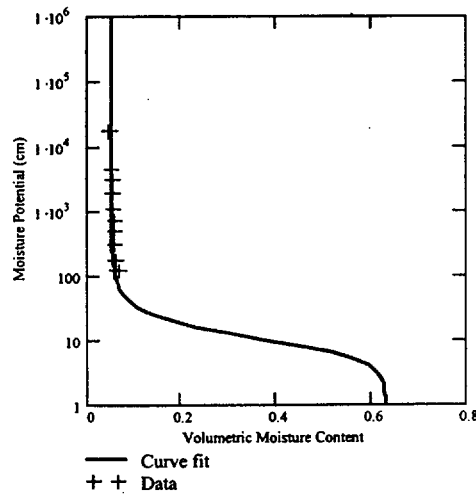
As discussed previously, the van Genuchten curve-fitting parameters were determined by fitting the curve to the retention data for crushed tuff (Section 4.1.5). Attachment IV, p. IV-22, presents the *Microsoft Excel 97* spreadsheet that uses the Equation Solver to calculate the curve-fitting parameters. The results from the curve-fitting process presented in Attachment IV, p. IV-22, are:

$$\theta_r = 0.05$$

$$\alpha_i = 0.12 \text{ (1/cm)}$$

$$n_i = 2.75$$

Figure 7 (Section 4.1.5) presents Equation (8) with the UFA data for the invert. Note that the measurements were performed near the residual moisture saturation. To establish the curve at higher moisture contents, the volumetric moisture content at saturation was estimated from the porosity. The volumetric moisture content θ_s equals the porosity of 0.63 which corresponds to the loose state (See Attachment IV, p. IV-13). It should be noted that while the UFA testing was performed on the crushed tuff in a loose state ($\phi = 0.63$) than what would be anticipated in the repository ($\phi = 0.55$) allowing for consolidation over time, the moisture retention scaled to the saturation level would not be significantly different.



Note: Refer to Section 6.2.2.2 for sieve sizes.

Figure 7. Moisture Retention Relationship for the Invert

6.2.2.4 Intrinsic Permeability

The saturated hydraulic conductivity (K_s) of the invert is estimated from the RETC curve fitting analysis presented in Attachment IV, pp. IV-25 to IV-28, using the combined UFA unsaturated hydraulic conductivity (K_u) to moisture potential (ψ) and retention measurements. The calculated value from the RETC analysis is 0.60 cm/sec. This value corresponds to an approximate intrinsic permeability conversion value of $6.0 \times 10^{-6} \text{ cm}^2$ (Freeze and Cherry, p. 29).

6.2.2.5 Relative Permeability

The UFA test apparatus described above was used to determine the relationship of unsaturated hydraulic conductivity (K_u) to volumetric moisture content (θ) for the invert. Figure 8 presents the data for comparison to the relationship presented in Equation (9) with van Genuchten curve-fitting parameters obtained from the retention relationship (Attachment IV, p. IV-13). Figure 9 presents the relationship of unsaturated hydraulic conductivity to moisture potential obtained from Equation (10) and the same curve-fitting parameters.

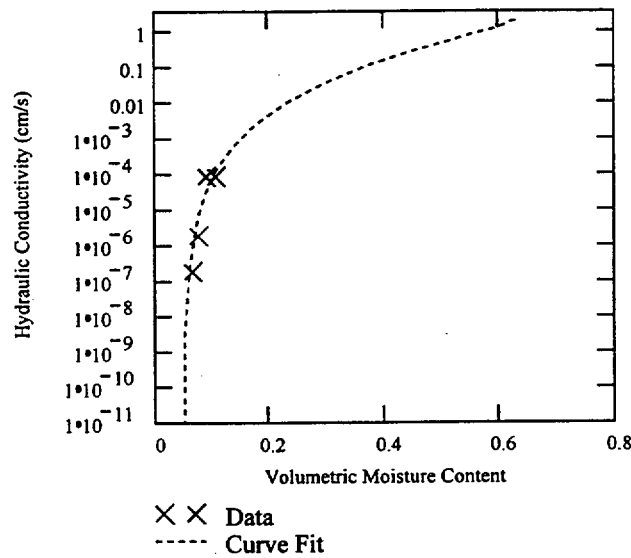


Figure 8. Unsaturated Hydraulic Conductivity versus Volumetric Moisture Content for the Invert

6.2.2.6 Material Thermal Properties

The invert is composed of crushed tuff as discussed previously. For such a cohesionless material, the thermal conductivity (K_i) is a strong function of water content (Jury et al. 1991, p. 183, Fig. 5.11a). For dry crushed tuff, the thermal conductivity is about 0.58 to 0.74 W/m-°K, or an average value of 0.66 W/(m-°K) (Ryder et al. 1996, p. 5-3). This value is similar to the dry sand thermal conductivity reported by de Marsily (1986, p. 281) of 0.4-0.8 W/(m-°K).

The rock grain specific heat for tuff is estimated to be 948 J/(kg*°K) (Section 4.1.4). The specific heat for the crushed tuff with a porosity of 0.55 and a bulk density of 1.15 g/cm³ equals the specific heat of the grains since specific heat capacity depends on mass which is independent of volume. The volumetric heat (C_p) equals the specific heat (C_s) 948 J/(kg °K) times the bulk density (ρ) 1.15 g/cm³. The thermal emissivity of the invert is assumed equal to the emissivity for quartz on a rough surface 0.93 (Holman 1997, p. 649).

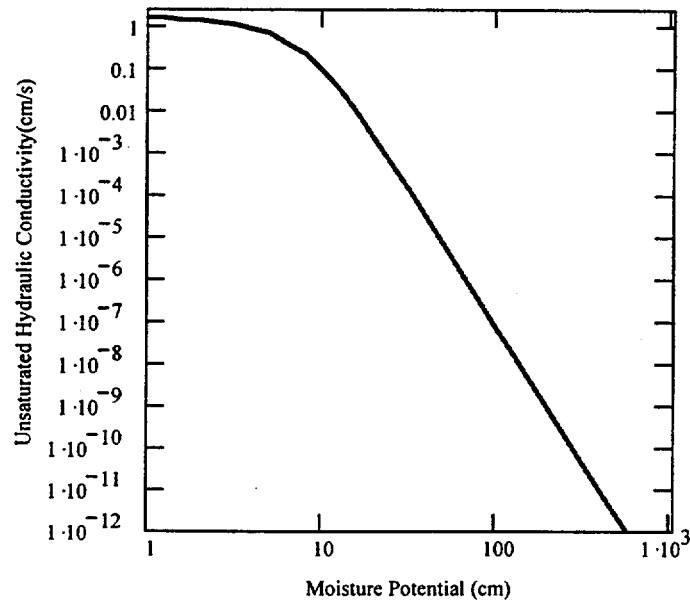


Figure 9. Unsaturated Hydraulic Conductivity versus Moisture Potential for the Invert

6.2.3 Properties of the Altered Invert

The potential exists for fines to move downward from the backfill into the invert outside of the drip shield. The retention and water flow characteristics of this material could also be governed by the grain size distribution for the combined materials.

Campbell (1985, pp. 43 to 47) presents a series of empirical relationships for determining the moisture retention curve from soil texture for well-graded materials having a simple, unimodal pore size distribution function. More complex materials can be thought of as mixtures of materials with these simple characteristics. The moisture characteristic of a mixture of porous materials is (Campbell, 1985, p. 46):

$$\theta = \sum \theta_i \cdot \phi_i \quad (\text{Eq. 16})$$

$$\theta = \sum \phi_i \cdot \psi_{a_i} \cdot \psi_i^{-\frac{1}{b_i}} \quad (\text{Eq. 17})$$

The expression presented above is a “weighting” function, which states that the retention relationship can be weighted on the basis of proportional grain sizes. The van Genuchten volumetric moisture content (θ) versus moisture potential (ψ) relationship can be weighted in equal proportions (Section 5.9). Equation (8) can then be used to plot a retention curve for the combined material. This curve is presented in Figure 10.

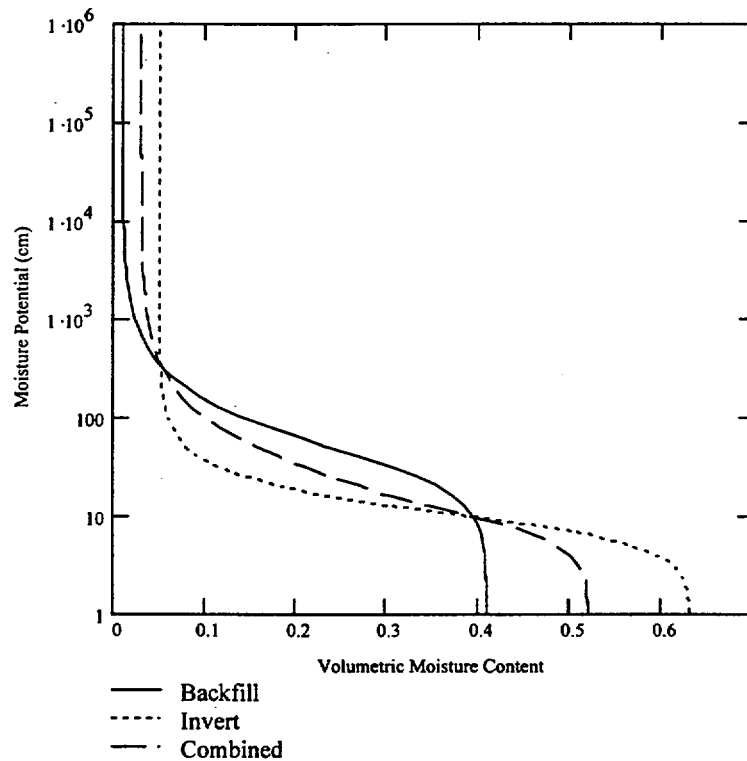


Figure 10. Moisture Retention Relationship for the Combined Material

Further, Attachment IV, pp. IV-23 to 24, presents an analysis of the van Genuchten parameters for the combined material. The results for the van Genuchten parameters are:

$$\theta_r = 0.03$$

$$\alpha_b = 0.104 \text{ cm}^{-1}$$

$$n_b = 1.85$$

The saturated hydraulic conductivity for flow in series of the mixture is governed by the harmonic mean of the saturated hydraulic conductivities (Freeze and Cherry 1979, p. 34) (Section 5.10):

$$K_c = \frac{L_1 + L_2}{\frac{L_1}{K_1} + \frac{L_2}{K_2}}$$

(Eq. 18)

The calculated harmonic mean for the intrinsic permeability (K_c) for the combined material, based upon the intrinsic permeabilities of the backfill and the invert, is $2.8 \times 10^{-11} \text{ m}^2$. This is equivalent to a hydraulic conductivity of 0.028 cm/sec that is weighted more to the finer texture of the Overton Sand. Figure 11 presents a plot of the relationship of unsaturated hydraulic conductivity to moisture potential using Equation 10, and the van Genuchten parameters presented above.

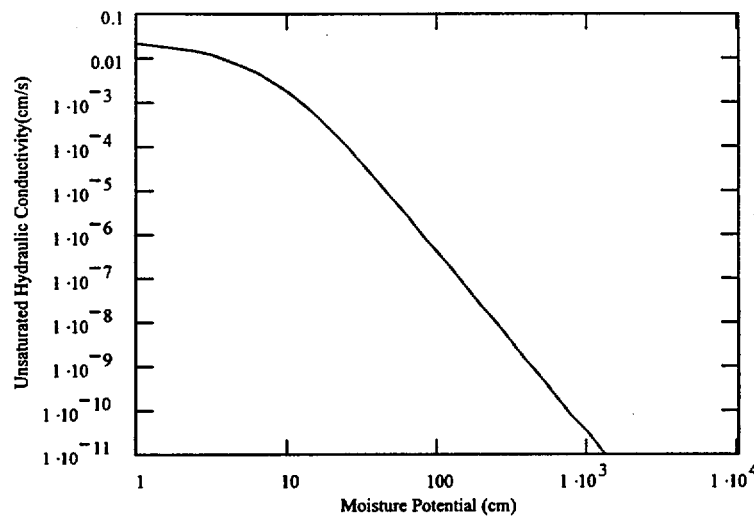


Figure 11. Unsaturated Hydraulic Conductivity versus Moisture Potential for a Combined Material

6.2.4 Hydrological Properties of the Drip Shield

As the drip shield “wets” up (becomes wetter), a fraction of the penetrations will be filled with water and become available for flow. The flow rate for a given head difference reduces to a small value when these pits or crevices are filled with water. This process will completely dominate the flow process under some conditions (Jury et al. 1991, p. 89). The following discussion develops a flow model to assess the dependence of the drip shield flow on the moisture potential.

The following analysis applies the capillary tube bundle model (Jury et al. 1991, pp. 91 to 92) to develop relationships between moisture potential and the flow rate divided by the head difference for the drip shield. A simple model for the drip shield water flow is developed using bundles of capillary tubes of different sizes. The capillary tube bundle theory is then extended to the case of crevices or apertures.

A hypothetical network of tubes in the drip shield that are circular in shape has a hydraulic head or potential applied across the flow path length (L_c) (Section 5.4). A hydraulic head gradient ΔH is placed across the ends of the column of tubes, causing water to flow (if water is present) through each of the capillary tubes according to Poiseuille's law. Thus, a single capillary of radius R_j has a volume flow rate Q_j given by (Jury et al. 1991, p. 90):

$$Q_j = \frac{\pi \cdot R_j^4 \cdot \rho_w \cdot g \cdot \Delta H}{8 \cdot \nu \cdot L_c} \quad (\text{Eq. 19})$$

The total flow Q_T through the column, when all tubes are filled with water without corrosion products, is (Jury et al. 1991, p. 90):

$$Q_T = \sum_{j=1}^M N_j \cdot Q_j \quad (\text{Eq. 20})$$

$$Q_T = \frac{\pi \cdot \rho_w \cdot g \cdot \Delta H}{8 \cdot \nu \cdot L_c} \cdot \sum_{j=1}^M N_j \cdot R_j^4 \quad (\text{Eq. 21})$$

In this analysis, N_j represents the number of capillaries of radius R_j in the bundle and M represents the number of different capillary size classes or categories in the bundle of tubes making up the column. Figure 12 presents a conceptual model for the probability density distribution that might represent the distribution of pit holes. Note that the actual probability density function and the scale of the probability function may be different from the concept shown here.

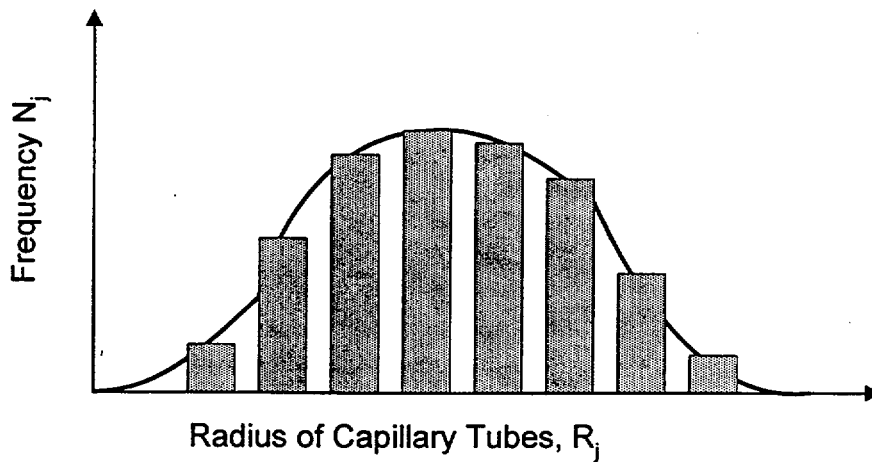


Figure 12. Concept for Distribution of Capillary Tube Bundles at Some Time

Let $[N_1, N_2 \dots N_n]$ represent a vector of the frequency of capillary tubes for the size classes, in ascending order, for the vector $[R_1, R_2 \dots R_n]$ presented in Figure 12. The elements of a moisture potential vector can be calculated by applying the capillary equation (Jury et al. 1991, p. 91) for the case of the wetting angle being equal to zero (Section 5.8):

$$R_j = \frac{2\sigma}{\rho_w g \psi_j} \quad (\text{Eq. 22})$$

Solve for the moisture potential (ψ_j) in terms of R_j :

$$\psi_j = -2 \frac{\sigma}{\rho_w g R_j} \quad (\text{Eq. 23})$$

The $[\psi_1, \psi_2 \dots \psi_n]$ represents a vector of moisture potential in ascending order since by the convention discussed previously, the moisture potential is negative. Considering the case of a moisture potential ψ_0 applied outside the drip shield and moisture potential ψ_i applied on the inside of the drip shield. If $\psi_i < \psi_0$, then water could form a water-solid boundary in some of the pore spaces (Section 5.5) and could be drawn in through the drip shield. Also, water could be

drawn in by gravity, though this component is limited to the thickness of the drip shield. The index j_T is defined as the index:

$$\psi_{j_T-1} < \psi_o < \psi_{j_T} \quad (\text{Eq. 24})$$

For capillaries where $\psi_j < \psi_o$, water is retained and flow occurs from the backfill to the waste package. The flow rate calculated from Equation (21), according to Poiseuille's Law above, then becomes:

$$Q_T = \sum_{j=1}^{j_T-1} \frac{\pi \cdot \rho_w \cdot g}{8 \nu \cdot L_c} \left[(\psi_o + z_o) - (\psi_j + z_j) \right] \cdot N_j \cdot R_j^4 \quad (\text{Eq. 25})$$

This expression can be rewritten in terms of the hydraulic gradient with flow in the vertical direction:

$$Q_T = \sum_{j=1}^{j_T-1} \frac{\pi \cdot \rho_w \cdot g}{8 \nu} \left(\frac{d}{dz} \psi + 1 \right) \cdot N_j \cdot R_j^4 \quad (\text{Eq. 26})$$

Similar expressions can be written for crevices by applying the parallel plate theory. Kwicklis and Healy (1993, p. 4094) developed a relationship for flow between parallel plates which can be derived as follows:

$$Q_j = \frac{1}{12 \cdot \nu} \cdot \frac{\Delta H \cdot \rho_w \cdot g}{L_c} \cdot B_j^3 \cdot w_c \quad (\text{Eq. 27})$$

Further, the retention relationship for the wetting angle being zero (Section 5.8) is given by (Kwicklis and Healy 1993, p. 4094):

$$\psi_j = \frac{-2\sigma}{\rho_w g B_j} \quad (\text{Eq. 28})$$

Let $[N_1, N_2 \dots N_n]$ represent a vector of the frequency capillary apertures of the vector $[B_1, B_2 \dots B_n]$ in ascending order. The elements of a moisture potential vector can be calculated by applying the capillary equation (Equation 28).

By applying the same technical approach, the flow through the parallel plate crevices can be calculated as

$$Q_T = \sum_{j=1}^{j_T-1} \frac{\rho_w g}{12 \nu \cdot L_c} [(\psi_o + z_o) - (\psi_i + z_i)] \cdot N_j \cdot B_j^3 \cdot w_c \quad (\text{Eq. 29})$$

This expression can be rewritten for flow in the vertical direction:

$$Q_T = \sum_{j=1}^{j_T-1} \frac{\rho_w g}{12 \nu} \left(\frac{d}{dz} \psi + 1 \right) \cdot N_j \cdot B_j^3 \cdot w_c \quad (\text{Eq. 30})$$

6.2.4.1 Moisture Potential Governed by Relative Humidity and Temperature Inside the Drip Shield

The tendency for water to be drawn in through the drip shield depends on the moisture potential on the inside surface of the drip shield. The moisture potential, in turn, depends on the relative humidity (RH) and absolute temperature (T) on the inside surface of the drip shield. At equilibrium, the vapor water potential equals the liquid water potential (Jury et al. 1991, p. 60). As the vapor and liquid phases are at essentially the same elevation, the relative humidity can be expressed as (Jury et al. 1991, p. 60):

$$RH = \exp\left(\frac{M_w \psi}{\rho_w R T}\right) \quad (\text{Eq. 31})$$

$$\psi = \frac{\rho_w R T}{M_w} \ln(RH) \quad (\text{Eq. 32})$$

Figure 13 presents a plot of the relationship of the moisture potential (ψ) to relative humidity from the relationship presented above. The moisture potential (ψ) is a strong function of relative humidity (RH), Equation 32, or the ratio of the vapor pressure (P_v) on the inside of the drip shield to the saturated vapor pressure (P_{vsat}) at temperature (T).

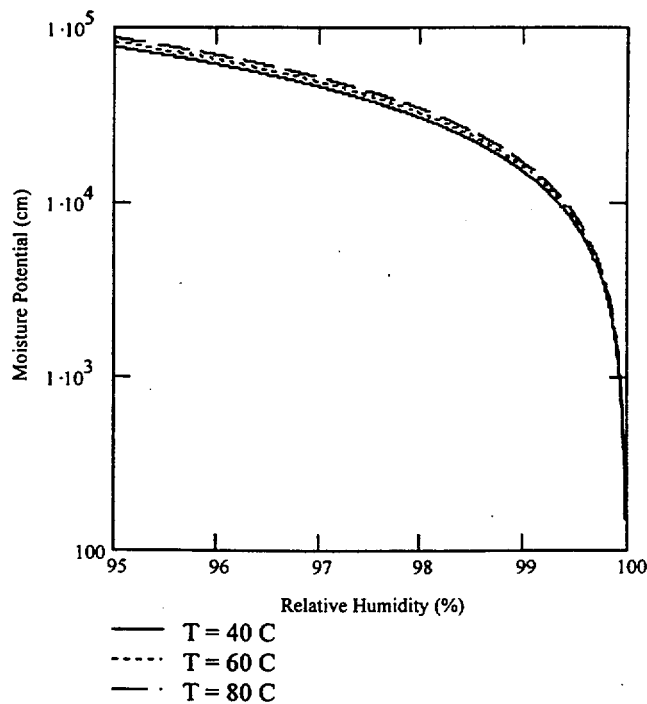


Figure 13. Relationship of Moisture Potential to Relative Humidity

6.2.4.2 Moisture Potential Governed By Capillary Retention in the Backfill Outside the Drip Shield

Philip et al. (1989, pp. 16 to 28) present a model for unsaturated seepage in subterranean holes. It consists of analyzing the exclusion problem for cylindrical cavities. Philip et al. (1989, p. 16) present a general theory of water exclusion from or entry into cylindrical cavities from a steady vertical seepage under unsaturated conditions. It is known that the drip shield acts to exclude water. If the hydraulic potential is calculated on the basis of the general theory of water exclusion, then the calculated water flow represents an upper bound to the hydraulic potential under ambient temperature conditions. This is because under static conditions of no flow, a maximum gradient would be maintained, while flow through the drip shield would tend to “draw down” the hydraulic potential, resulting in a reduced gradient.

Philip et al. (1989, p. 17) developed a solution for the Kirchhoff Potential (Θ) for a quasi-linear flow equation. The Kirchhoff Potential at some arbitrary point is defined as:

$$\Theta = \int_{-\infty}^{\psi} K d\psi \quad (\text{Eq. 33})$$

Two special values of Θ are introduced:

$$\Theta_0 = \int_{-\infty}^{\psi_0} K d\psi \quad (\text{Eq. 34})$$

$$\Theta_1 = \int_{-\infty}^0 K d\psi \quad (\text{Eq. 35})$$

Phillip used these definitions to describe boundary conditions for subcritical, critical, and supercritical regimes. Consider boundary conditions on the domain of the backfill. Far from the cavity surface (r approaches ∞), the potential function Θ approaches Θ_0 for steady downward flow. The second boundary condition is at the cavity surface for incipient flow into the cavity. For no flow to enter through the drip shield, Θ is less than or equal to Θ_1 on the cavity surface.

Philip et al. (1989, p. 18) solve a quasi-linear flow equation by considering an exponential representation of $K(\psi)$. For many quasi-linear flow systems, the exponential representation is fitted optimally to a finite range of ψ . The exponential distribution used to express the relationship of unsaturated hydraulic conductivity to moisture content is (Philip et al. 1989, p. 18):

$$K(\psi) = K_0 \cdot e^{\alpha \cdot (\psi - \psi_0)} \quad (\text{Eq. 36})$$

For Overton Sand, the exponential function presented in Attachment V is fit to the data over the approximate range of the moisture potential (ψ) from 0 to about -440 cm, corresponding to a range of the absolute value of suction pressure from 0.0 to 0.44 bars (Figure 14), as discussed below. The constant α is estimated to be 0.027 cm^{-1} (See Attachment IV, p. IV-10).

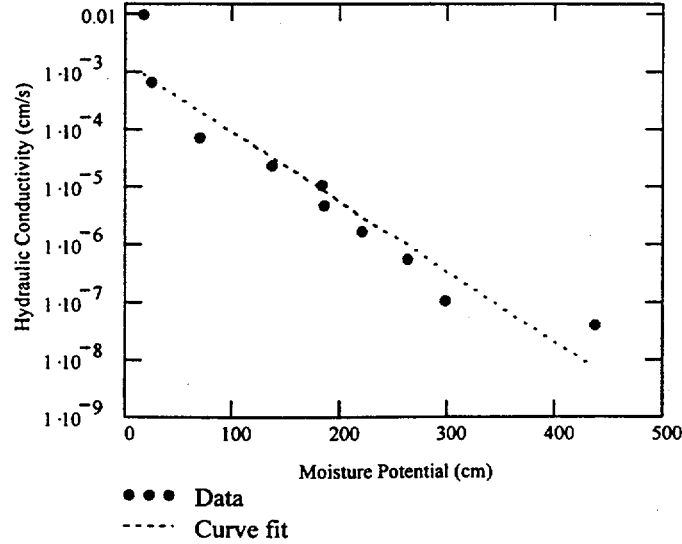


Figure 14. Relationship of Hydraulic Conductivity to Moisture Potential Using the Exponential Relationship

Project design descriptions have been developed for the maximum percolation flux of 25 mm per year at the repository horizon (Section 5.13). If consideration is given to the unsaturated hydraulic conductivity of the backfill, for the case of steady state flow in a deep water table (Jury et al. 1991, p. 127), the moisture potential in the backfill can be solved from Equation (10) by setting the unsaturated hydraulic conductivity equal to approximately 8×10^{-8} cm/sec. The approximate value of the moisture potential is -360 cm.

Philip et al. (1989, p. 18) define a variable I that represents the ratio of the Kirchhoff Potential Θ at some point in the media to the reference Θ_0 . A closed form solution is presented for a cylindrical cavity of diameter l in terms of a dimensionless parameter (s) (Philip et al. 1989, p. 20):

$$s = \frac{\alpha l}{2} \tag{Eq. 37}$$

$$I(s, r, \zeta) := 1 + 4e^{sr \cos(\zeta)} \left[\sum_{j=1}^{20} \frac{j \text{In}(j, s)}{K_n(j, s)} K_0(sr) \dots + \sum_{n=1}^{20} (-1)^n K_n(n, s, r) \cos(n \zeta) \left(\frac{n \text{In}(n, s)}{K_n(n, s)} + 2.0 \sum_{j=n+1}^{20} \frac{j \text{In}(j, s)}{K_n(j, s)} \right) \right] \tag{Eq. 38}$$

Note that $In(j,s)$ and $Kn(j,s)$ are modified Bessel functions of the first and second kind (Philip et al. 1989, p.19). The indices i and j are used in the series summations. Also, note that Equation 38 with the evaluation of 20 terms provides a solution that is in agreement with the results in p. 22 of Philip et al. 1989.

As s approaches zero, capillarity dominates, whereas as s approaches infinity, gravity dominates. A solution for the ratio I is presented by Philip et al. (1989, p. 20) as shown in Figure 15.

Figure 15 presents an analysis of the drip shield with an approximate value of $s = 3.3$ from Equation (37) based upon $\alpha = 0.027 \text{ cm}^{-1}$ (See Attachment IV, p. IV-10) for a drip shield diameter of 246.2 cm (Section 4.1.1). This figure is in agreement with the potential contours shown by Philip et al. (1989, p. 22). The figure shows that around the drip shield, the potential is increased with a drip lobe ($I > 1$) forming to the side and above of the drip shield, and a dry shadow forming below the drip shield ($I < 1$). The presence of the drip shield increases the moisture content everywhere outside the dry shadow above and to the side of the drip shield.

The maximum values for I can be calculated from Equation 38 by noting that I is maximized when the dimensionless radius is 1 and ζ equals π (Philip et al. 1989, p. 20). In the case of the drip shield, the maximum ratio of I is approximately 8 (Attachment V, p. V-5). The moisture potential ψ can be solved for approximately -280 cm. Therefore, the fine Overton Sand backfill provides for capillarity and the moisture potential for solving the exclusion problem changes from approximately -360 cm to -280 cm. The Overton Sand provides for capillarity, and reduces the potential for the formation of free water on the drip shield.

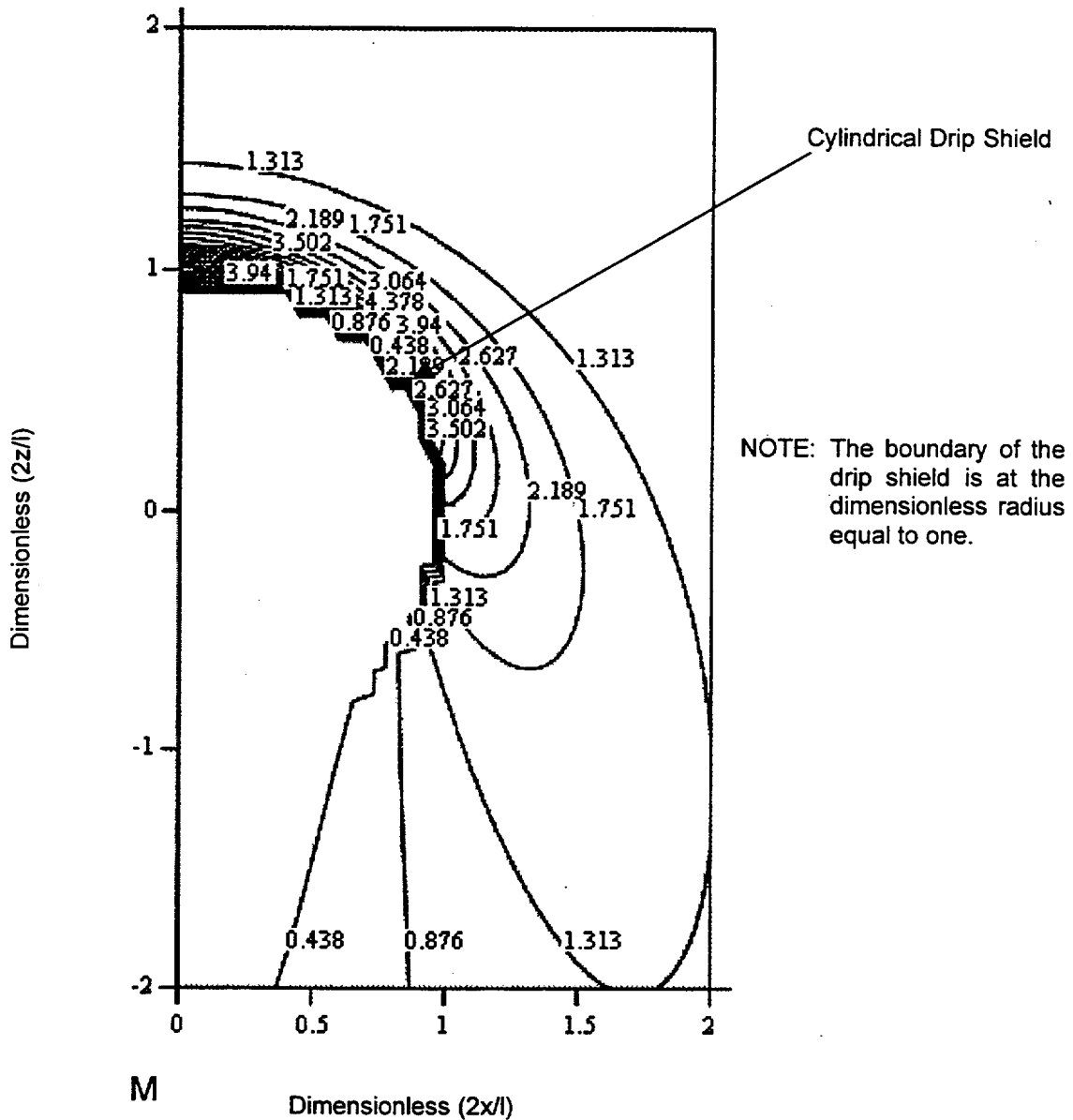


Figure 15. Seepage About Cylindrical Drip Shield

6.2.5 Bounding Calculation for the Drip Shield

The drip shield design is under development and is out of the scope of this document. The drip shield design currently shows that the length of each individual drip shield is 5,485 mm long or 5.485 m long (Section 4.1.6). The placement of drip shields end to end would result in multiple interior joints between the drip shields. For the current design, the drip shields are placed with an overlap over each joint (Section 5.12). The geometry of the flow path can be identified (Section 5.6).

The equations and analyses in the previous sections can be used to bound the flow conductance through the drip shield. Equations (21) and (30) express the flow rate as a function of the moisture potential for circular pits, and parallel plates, respectively. These relations reflect the degree to which capillary structures through the drip shield retain and transmit water through the drip shield.

In future analyses, equivalent continuum or dual continuum models using NUFT will be developed in two and three dimensions using either an equivalent continuum model (ECM) or a discrete fracture model. The following analyses present bounding calculations for the flow conductance for these two models.

An aperture between the overlapping drip shields is characterized by a moisture potential ψ . Equation (28) can be rewritten to express the relation of the largest aperture that could retain water to the absolute value of moisture potential ψ :

$$B = \frac{2\sigma}{\rho_w g \psi} \quad (\text{Eq. 39})$$

According to (Section 5.7), the analysis assumes that the physical aperture equals the aperture that maximizes flow rate. In other words, the aperture between the overlapping joint and the drip shield is assumed to be uniform, and equal the aperture from Equation (39). Thus, $B_1 = B_2 = \dots B_N = B$, the uniform aperture is filled with water ($j_T = 2$), and the width of the aperture (w_c) equals the wetted perimeter for the overlapping joint ($P = w_c$). Substituting Equation (39) into Equation (27) at the same elevation gives:

$$Q_T = \frac{\rho_w g}{12 \cdot \nu} \cdot \left(\frac{\psi_i - \psi_o}{L_c} \right) \cdot \left(\frac{2 \cdot \sigma}{\rho_w g \psi} \right)^3 \cdot P \quad (\text{Eq. 40})$$

Consider that an equivalent conductivity is selected for the drip shield that is equal to this function over the peripheral area of the drip shield. The peripheral area of the drip shield is taken as the arc length along the sides and top of the drip shield (P) times the length of the drip shield (L_{DS}). Writing Darcy's Law for the flow rate over the drip shield (Jury et al., 1991, p. 94):

$$Q_T = K(\psi) \frac{(\psi_i - \psi_o)}{\Delta t} L_{DS} P \quad (\text{Eq. 41})$$

Then, by equating Equations 40 and 41, the equivalent unsaturated conductivity for the Equivalent Continuum Model can be written as:

$$K(\psi) = \frac{\rho_w g}{12 \cdot \nu} \cdot \left(\frac{\Delta t}{L_c} \right) \cdot \left(\frac{2 \cdot \sigma}{\rho_w g \psi} \right)^3 \cdot \frac{1}{L_{DS}} \quad (\text{Eq. 42})$$

Substituting the constants into Equation 42 for a nonwetting material and the geometry of the drip shield, the relationship of $K(\psi)$ to the moisture potential ψ can be determined (Attachment IV) as shown in Figure 16. The bounding curve for the drip shield can be compared to the unsaturated hydraulic conductivity for the backfill. The curve plots below the relationship

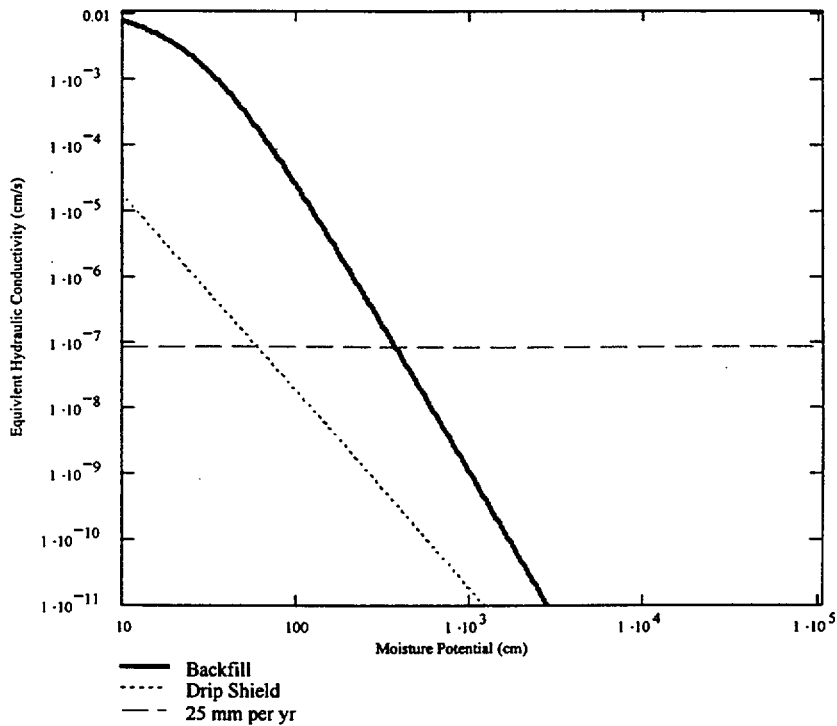


Figure 16. Bounding Relationship of the Equivalent Conductivity for the Drip Shield to Moisture Potential

for the backfill given by Equation (10) for the Overton Sand. Therefore, the drip shield provides a barrier to flow in the same manner as a coarse gravel (Webb 1997, p. 1855).

6.3 CONCEPTUAL FLOW DIVERSION MODEL BASED UPON CLOSED-FORM ANALYTICAL SOLUTIONS

The properties of the engineering components developed in the previous sections provide the basis for performing NUFT calculations to assess the partitioning of flow. As an alternative to performing NUFT calculations, a conceptual model and its mathematical basis using closed-form analytical solutions at isothermal temperature is developed (Section 5.14) and is presented below.

This model could be used with other models in performing Monte Carlo simulations. One reason for adopting a model based upon closed form analytical solutions is that changes in moisture potential (ψ) can result in large changes in unsaturated hydraulic conductivity that dominate performance. A model based upon more degrees of freedom and a more accurate geometry would not significantly increase accuracy over a simpler model.

Bear (1972, pp. 710 to 715) discusses the solution of the steady state and transient flow problems using a network resistance model. A steady one-dimensional flow through a sand column can be simulated with an array of resistors in which flow continuity is maintained at every node.

In this simple flow model, shown in Figure 17, the in-drift seepage (Q) is applied at Node 1, representing the point at which incoming flow occurs. The moisture potential (ψ) boundary condition equals to approximately -360 cm (Attachment VI, p. VI-4) is applied to Node 4. The model conservatively assumes that flow occurs immediately above the WP (Section 5.11). The flow from Node 1 to Node 4, and from Node 1 to Node 5, represents the flow through the backfill to the invert adjacent to the drip shield and through the drip shield, respectively. Node 6 is maintained at a moisture potential governed by the temperature (T) and relative humidity (RH) conditions below the drip shield, as shown in Equation (31). For steady unsaturated flow from node i to node j , Bear (1972, p. 504) presents the following integral equation:

$$\int_{s_i}^{s_j} 1 ds = \int_{\psi_i}^{\psi_j} \frac{1}{\frac{q_{ij}}{K(\psi)} + \sin(\alpha_{ij})} d\psi \quad (\text{Eq. 43})$$

or in terms of flow rate:

$$\int_{s_i}^{s_j} 1 ds = \int_{\psi_i}^{\psi_j} \frac{1}{\frac{Q_{ij}}{A_{ij} \cdot K(\psi)} + \sin(\alpha_{ij})} d\psi \quad (\text{Eq. 44})$$

Note that Q_{ij} is the branch flow rate from node i to j in the network resistance model.

The integral equation is written because the unsaturated hydraulic conductivity for the backfill in Equation (10) is a nonlinear function of the absolute value of moisture potential (ψ).

In the simple resistance model that invokes symmetry (Figure 17), the backfill flow above the drip shield is conservatively assumed to be in the vertical direction, with the flow directed

towards the drip shield. For the drip shield flow from Node 5 to Node 6 through the overlapping portion of the connector assembly, Equation (40) can be rewritten in differential form as:

$$Q = \frac{\rho_w \cdot g}{12 \cdot v} \left[\left(\frac{d}{ds} \psi \right) \cdot \left(\frac{2 \cdot \sigma}{\rho_w \cdot g \cdot \psi} \right)^3 \cdot P \right]$$

(Eq. 45)

or in integral form:

$$\int_{s_i}^{s_j} ds = \frac{\rho_w \cdot g \cdot P}{12 \cdot v \cdot Q_{ij}} \int_{\psi_i}^{\psi_j} \left(\frac{2 \cdot \sigma}{\rho_w \cdot g \cdot \psi} \right)^3 d\psi$$

(Eq. 46)

For the network resistance model shown in Figure 17, the branch flow rates Q_{12} , Q_{15} , Q_{23} , Q_{34} , and Q_{56} , and the moisture potential ψ_1 , ψ_2 , ψ_3 , and ψ_5 , constitute nine unknowns. Four branch flows using Equation (44), one branch flow using Equation (46) for flow through the drip shield, and four flow continuity equations at Nodes 1, 2, 3, and 5, can be written for the specified boundary condition of seepage flow at Node 1 (Section 5.11), and known moisture potentials (ψ_4 and ψ_6) at Nodes 4 and 6. The nonlinear equation solver in *Mathcad 8* (MathSoft 1998, p. 189) can be used to solve this system of equations.

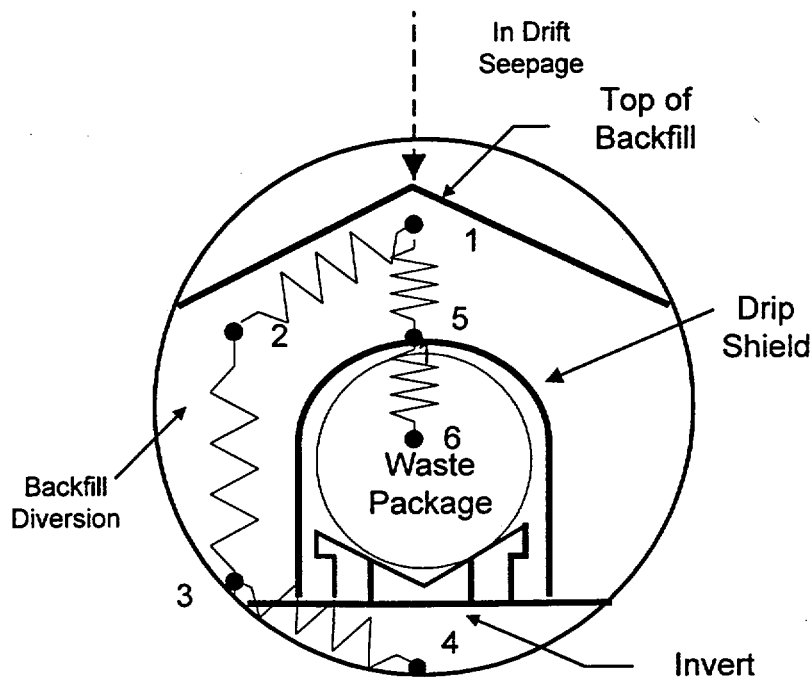


Figure 17. Conceptual Network Resistance Model for the Water Diversion Model

7. CONCLUSIONS

This AMR presents the geotechnical and hydrologic properties for the backfill, the invert, and the combined material (Section 6.2). These properties were incorporated in the conceptual network resistance model. The specific properties included grain size distribution, dry bulk density and porosity, moisture retention, intrinsic permeability, relative permeability and material thermal properties. The van Genuchten curve fit parameters were determined from a least squares fit to the measured UFA retention data for the Overton Sand with a gradation from 0.1 to 1 mm, and for crushed tuff with a gradation from 2.0 to 4.75 mm. An analysis was performed to estimate the hydrologic properties of the combined material. In addition, the estimated thermal properties for the materials were presented.

The hydrologic properties of the drip shield were presented based upon a capillary tube bundle model (Section 6.2.4). A hypothetical network of tubes, crevices or apertures is postulated and flow relationships presented based upon Poiseuille's Law for flow through a capillary tube or the Cubic Law for Flow Through Parallel Plates. These fundamental relationships provide the basis for estimating flow through existing apertures at the overlapping joints between drip shields or for pits and crevices that might develop due to drip shield degradation during the postclosure period.

The moisture potential governed by relative humidity and temperature inside the drip shield was presented that relates the moisture potential to the RH and T environment in the annulus between the drip shield and the waste package. The moisture potential is a strong function of the relative humidity (RH) or the ratio of the vapor pressure (P_v) on the inside of the drip shield to the

saturated vapor pressure (P_{vsat}) at temperature (T). The moisture potential on the outside of the drip shield in the backfill was estimated on the basis of a general theory of water exclusion or entry into cylindrical cavities from a steady vertical seepage under unsaturated conditions. Under the worst case assumption for percolation flux, the solution to the exclusion problem shows that the moisture potential in the Overton Sand changes from approximately -360 cm to -280 cm (Section 6.2.4.2). The Overton Sand provides for capillarity and reduces the potential for the formation of free water in the drip shield.

A bounding calculation was performed to estimate the diversion of flow around the drip shield (Section 6.2.5). The bounding calculation evaluated the flow conductance through the aperture between overlapping drip shields, and compared this to the unsaturated hydraulic conductivity of the backfill. Under the assumption of a 10-cm overlap with the flow path length equal to this length, the drip shield provides a potential barrier to flow in the same manner as a coarse gravel (Webb 1997, p. 1855).

The purpose of this AMR was to develop a conceptual model and constitutive relations to be used for bounding the volume of seepage water that is partitioned into (1) water flow through the drip shield that contacts the waste packages; (2) water flow that flows through the backfill directly to the invert; and (3) water flow that contacts the drip shield but does not flow through the drip shield. The properties of the engineering components developed in the previous sections provide the basis for performing NUFT calculations to assess the partitioning of flow. As an alternative to performing NUFT calculations, a conceptual model and its mathematical basis using closed-form analytical solutions at isothermal temperature was developed (Section 6.3). A simple resistance model that invokes symmetry was developed. This model can be used to solve for the flow rates through the branches, and the moisture potential at internal nodes. A system of non-linear equations can be solved based upon flow equations through each branch and flow continuity equations at internal nodes.

The results of this model are based on unqualified technical information and unqualified software (TBV-3924). Therefore, use of any unqualified technical information or results from this model as input in documents supporting construction, fabrication, or procurement, or as part of a verified design to be released to another organization, is required to be identified and controlled in accordance with appropriate procedures.

The impact of TBVs on conclusions is categorized as follows:

- TBV – 3805 involve the use of empirical relationships in equal weighting (Section 5.9) for selection of the retention and flow properties of the combined material. This TBV may have some impact since a contrast in properties between the combined material and the invert may alter flow in the invert.
- TBV – 3806 involves the calculation of the saturated hydraulic conductivity of the combined material as equal to the harmonic mean for the backfill and invert materials (Section 5.10). These inputs and assumptions are preliminary, and would need to be confirmed. This TBV may have some impact since the contrast in hydraulic properties between the crushed tuff invert and backfill will influence flow rates in the invert.

- TBV – 3797, TBV – 3799, TBV – 3810 involve identifying the crushed tuff as the invert source material (Section 5.1) and using or developing the hydrologic and geotechnical properties for this material. These TBVs may have some impact on hydrologic analyses since these properties influence the predicted saturation levels in the invert.
- TBV-3924 involves the RETC result for the saturated hydraulic conductivity of the invert. This TBV may have some impact on hydrologic analyses since this property influences the predicted saturation levels in the invert.
- TBV – 3518, TBV – 3811, TBV – 3471 involves identifying the Overton Sand as the backfill material (Section 5.2) and using hydrologic and geotechnical properties data set for this material. These data are currently unqualified. This TBV may have some impact on hydrologic analyses since these properties influence the predicted saturation levels in the backfill.
- TBV – 3471 involves the tabulated in-drift geometric and thermal properties used in Drift Scale Models for the TSPA/SR. It is expected that these properties would impact hydrologic and thermal analyses.
- TBV – 3796, TBV – 3471 involves the drip shield design features. This drip shield design is under development, and is out of the scope of this document. It is expected that certain design features such as the length of the overlap of joints the drip shield length and thickness, would have some impact, while other features, such as the actual shape of the drip shield, would have minimal impact.
- TBV – 3800 involves the assumption (Section 5.4) that all capillary tubes or crevices (due to pitting or crevice corrosion) in the model are assumed to have the same length, which is equal to the thickness of the drip shield. It is expected that this assumption would have minimal impact.
- TBV – 3801 involves the assumption (Section 5.5) of water flow boundaries composed entirely of solid-water boundaries. It is expected that this assumption would have some impact on the water flow.
- TBV – 3803 involves the assumption (Section 5.6) of water flow through the interface of the drip shield overlap, at a specific moisture potential that is a function of the moisture retention and flow characteristics of the aperture. It is expected that this assumption would have some impact on the water flow in hydrologic analyses.
- TBV – 3802 involves the assumption (Section 5.7) of the parallel plate model for flow through the drip shield. It is expected that this assumption would have some impact on the water flow in hydrologic analyses.
- TBV – 3807 involves the assumption (Section 5.11) of the flow entering the drift from seepage that is assumed to enter immediately above the waste package. It is expected that this assumption would have some impact on the water flow in hydrologic analyses.

- TBV – 3808 involves the corrosion of the drip shield (Section 5.12). It is expected that this assumption will impact the post closure performance of the drip shield since pits and crevices can provide fluid pathways.
- TBV – 3312 involves the maximum percolation rate at the repository horizon. It is expected that this assumption may impact the analysis presented in this AMR for moisture potential in the backfill.
- TBV – 3809 involves the assumption of steady state flow. It is not expected that this assumption would impact hydrologic analysis.

The sources of uncertainty in the conceptual Water Diversion Model include the uncertainty in hydrologic properties for the backfill, the invert, and the drip shield; variability in drift seepage rates, and variability in corrosion properties. The Monte Carlo simulation methods discussed previously in Section 6.1 provides a means of addressing these uncertainties.

8. REFERENCES

8.1 DOCUMENTS CITED

Bear, J. 1972. *Dynamics of Fluids in Porous Media*. New York, New York: Dover Publications. TIC: 217568.

Campbell, G. S. 1985. "Soil Physics with BASIC Transport Models for Soil-Plant Systems," *Developments in Soil Science 14*. Amsterdam, The Netherlands: Elsevier Science B. V. TIC: 214477.

CRWMS M&O (Civilian Radioactive Waste Management System Management and Operating Contractor) 1996. *Engineered Barrier System Performance Requirements Systems Study Report*. BB0000000-01717-5705-00001 REV 01. Las Vegas, Nevada: CRWMS M&O. ACC: MOL.19970407.0169.

CRWMS M&O 1997. *Determination of Available Volume for Repository Siting*. BCA000000-01717-0200-00007 REV 00. Las Vegas, Nevada: CRWMS M&O. ACC: MOL.19971009.0699.

CRWMS M&O 1998. *Ex-Container System Description Document*. BCA000000-01717-1705-00019 REV 00. Las Vegas, Nevada: CRWMS M&O. ACC: MOL.19981117.0424.

CRWMS M&O 1999a. *Classification of the MGR Ex-Container System*. ANL-XCS-SE-000001 REV 00. Las Vegas, Nevada: CRWMS M&O. ACC: MOL.19990928.0221

CRWMS M&O 1999b. *Engineered Barrier System Performance Modeling (WP# 12012383MX)*. Activity Evaluation. Las Vegas, Nevada: CRWMS M&O. ACC: MOL.19990719.0317.

CRWMS M&O 1999c. *Development Plan for Water Diversion Model*. TDP-EBS-MD-00012 REV 02. Las Vegas, Nevada: CRWMS M&O. ACC: MOL.19991118.0182.

CRWMS M&O 1999d. *Drip Shield Design*. Design Input Transmittal EBS-WP-99292.T. Las Vegas, Nevada: CRWMS M&O. ACC: MOL.19991014.0107.

CRWMS M&O 1999e. *Waste Package Design and Corrosion Information Engineered Barrier System Organization (EBSO) – Water Diversion Model and Radionuclide Transport Models*. Design Input Transmittal EBS-WP-99244.T. Las Vegas, Nevada: CRWMS M&O. ACC: MOL.19991018.0167.

CRWMS M&O 1999f. *Planning Guidance for EBS Test Number 3 – Drip Shield Test*. Memo from J. Pye to Distribution. LV.EBSPMJHP.05/99-005. Las Vegas, Nevada: CRWMS M&O. ACC: MOL.19990518.0308.

de Marsily, G. 1986. *Quantitative Hydrogeology – Groundwater Hydrology for Engineers*. San Diego, California: Academic Press. TIC: 208450.

DOE (U.S. Department of Energy) 1998a. *Quality Assurance Requirements and Description*. DOE/RW-0333P, Rev 8. Washington, D.C.: U.S. Department of Energy Office of Civilian Radioactive Waste Management. ACC: MOL.19980601.0022.

DOE 1998b. *Total System Performance Assessment. Volume 3 of Viability Assessment of a Repository at Yucca Mountain*. DOE/RW-0508. Washington, D.C.: U.S. Department of Energy, Office of Civilian Radioactive Waste Management. ACC: MOL.19981007.0030.

Fetter, C.W. 1993. *Contaminant Hydrogeology*. New York, New York: Macmillan Publishing Co. TIC: 240691.

Freeze, R. A. and Cherry J. A. 1979. *Groundwater*. Englewood Cliffs, New Jersey: Prentice-Hall, Inc. TIC: 217571.

Holman, J.P. 1997. *Heat Transfer*, Eighth Edition. New York, New York: McGraw Hill Book Co. TIC: 239954.

Jury, W. A.; Gardner, W.R.; and Gardner, W.H. 1991. *Soil Physics*, Fifth Edition. New York, New York: John Wiley & Sons. TIC: 241000.

Kwicklis, E. M. and R. W. Healy. 1993. "Numerical Investigation of Steady Liquid Water Flow in a Variably Saturated Fractured Network." *Water Resources Research* 29 (12), pp. 4091-4102. Washington D.C.: American Geophysical Union. TIC: 226993.

Lide, D.R., and Frederikse, H. P. R. eds. 1997. *CRC Handbook of Chemistry and Physics*, 78th Edition. Boca Raton, Florida: CRC Press. TIC: 243741.

MathSoft 1998. *Mathcad 8, User's Guide*. Cambridge, Massachusetts: MathSoft Inc. TIC: 242289.

Philip, J.R. Knight, J.H., and Waechter, R. T. 1989. "Unsaturated Seepage and Subterranean Holes: Conspectus, and Exclusion Problem for Circular Cylinder Cavities." *Water Resources Research*, 25 (1), pp. 16-28. Washington D.C.: American Geophysical Union. TIC: 239117.

Ryder, E.E.; Finley, R.E.; George, J.T.; Ho, C.K.; Longenbaugh, R.S.; and Connolly, J.R. 1996. *Bench-Scale Experimental Determination of the Thermal Diffusivity of Crushed Tuff*. SAND94-2320 Albuquerque, New Mexico.: Sandia National Laboratories. MOL.19961111.0011.

van Genuchten, M.T; Leij F.J. and Yates, S.R. 1991. *The RETC Code for Quantifying the Hydraulic Functions of Unsaturated Soils*. EPA Report 600/2-91/065. Riverside California:, U.S. Salinity Laboratory, U.S. Department of Agriculture. TIC: 236938.

Webb, S.W. 1997. *Generalization of Ross' Tilted Capillary Barrier Diversion Formula for Different Two-Phase Characteristic Curves*. *Water Resources Research*, 33, (8), pp. 1855-1859. Washington, D.C.: American Geophysical Union. TIC: 240311.

Wilkins, D.R. and Heath, C.A. 1999. "Direction to Transition to Enhanced Design Alternative II." Letter from Dr. D.R. Wilkins and C.A. Heath (CRWMS M&O) to Distribution, June 15, 1999, LV.NS.JLY.06/99-026, with enclosures. "Strategy for Baseline EDA II Requirements" and "Guidelines for Implementation of EDA II." ACC: MOL.19990622.0126; MOL.19990622.0127; MOL.19990622.0128.

8.2 CODES, STANDARDS, REGULATIONS, AND PROCEDURES

AP-2.13Q, Rev. 0, ICN 1. *Technical Product Development Planning*. Washington D.C.: U.S. Department of Energy, Office of Civilian Radioactive Waste Management. ACC: MOL.19991115.0230.

AP-3.10Q, Rev. 1, ICN 1. *Analyses and Models*. Washington, D.C.: Department of Energy, Office of Civilian Radioactive Waste Management. ACC: MOL.19991019.0467.

AP-3.15Q, Rev. 0, ICN 2. *Managing Technical Product Inputs*. Washington D.C.: U.S. Department of Energy, Office of Civilian Radioactive Waste Management. ACC: MOL.19991123.0068.

AP-SI.1Q, Rev. 2, ICN 1. *Software Management*. Washington D.C.: U.S. Department of Energy, Office of Civilian Radioactive Waste Management. ACC: MOL.19991101.0212.

QAP-2-0, Rev. 5. *Conduct of Activities*. Las Vegas, Nevada: Civilian Radioactive Waste Management System Management and Operating Contractor (CRWMS M&O). ACC: MOL.19980826.0209.

QAP-2-3, Rev 10. *Classification of Permanent Items*. Las Vegas, Nevada: Civilian Radioactive Waste Management System Management and Operating Contractor (CRWMS M&O). ACC: MOL.19990316.0006.

8.3 SOURCE DATA

SN9908T0872799.004. Tabulated In-Drift Geometric and Thermal Properties Used in Drift Scale Models for TSPA/SR (Total System Performance Assessment-Site Recommendation). Submittal Date: 8/30/1999.

GS980808312242.015. Water Retention And Unsaturated Hydraulic Conductivity Measurements For Various Size Fractions Of Crushed, Sieved, Welded Tuff Samples Measured Using A Centrifuge. Submittal Date: 08/21/1998.

MO9901YMP98017.001. Fracture Flux at Repository For QB.OUT. Submittal Date: 01/05/1999.

MO9912EBSPWR28.001. Particle Size Data, Water Retention Data, and Hydraulic Conductivity Data for Overton Sand Used in the Water Diversion Model AMR (ANL-EBS-MD-000028 REV 00). Submittal Date: 12/02/1999.

9. ATTACHMENTS

Attachment	Title
I	This section is reserved
II	Acronyms and Abbreviations
III	List of Symbols
IV	Moisture Retention Characteristics of the Backfill and Invert Materials
V	Flow Exclusion Analysis
VI	Bounding Analysis for a Drip Shield

ATTACHMENT I
THIS SECTION IS RESERVED

ATTACHMENT II
ACRONYMS AND ABBREVIATIONS

ATTACHMENTS II
ACRONYMS AND ABBREVIATIONS

AMR	Analysis and Modeling Report
CRWMS	Civilian Radioactive Waste Management System
DOE	United States Department of Energy
DS	Drip Shield
DTN	Data Tracking Number
EBS	Engineered Barrier System
EBSO	Engineered Barrier System Operations
ECM	Equivalent Continuum Model
EDA	Enhanced Design Alternative
LADS	License Application Design Selection
M&O	Management and Operating Contractor
MGR	Mined Geologic Repository
NF	Near Field
NUFT	Non-isothermal Unsaturated Saturated Flow and Transport
PMR	Process Model Report
QAP	Quality Assurance Plan
QARD	Quality Assurance Requirements and Description
RETC	RETention and Conductivity Fitting Curve
RH	Relative Humidity
SR	Site Recommendation
T	Temperature
TBV	To Be Verified
THC	Thermal-Hydrologic-Chemical

Ttp1l	Topopah Spring Tuff: Crystal-poor Lower Nonlithophysal Zone
Ttpmn	Topopah Spring Tuff: Crystal-poor Middle Nonlithophysal Zone
TSw2	Topopah Spring Thermal Mechanical Unit
UFA	Unsaturated Flow Apparatus
USGS	United States Geological Survey
WAPDEG	Waste Package Degradation Model
WP	Waste Package

**ATTACHMENT III
LIST OF SYMBOLS**

ATTACHMENT III LIST OF SYMBOLS

Units of Measurement

°	=	angle in degrees
°C	=	degree Celsius
cal	=	calorie
cm	=	centimeter
g	=	gram
kg	=	kilogram
hr	=	hour
J	=	joule
°K	=	kelvin
l	=	liter
m	=	meter
ml	=	milliliter
mm	=	millimeter
N	=	newton
Pa	=	pascal
sec	=	second
W	=	watt
yr	=	year

Lower Case Arabic Variables

b_i	=	Constant for the i th component of the soil
b_0, b_1	=	Constants from the linear regression analysis
g	=	Acceleration due to gravity (cm^2/sec)
i	=	index variable
j	=	Index for capillary tubes or parallel plate crevices
j_T	=	Index for which ψ_{jT}
l	=	cavity diameter
$\log h$	=	log variable for defining a vector of points for plotting
m	=	$1-1/n$, van Genuchten parameter for two parameter model
n	=	van Genuchten curve-fitting parameter
q_{ij}	=	Flux rate from node i to j in the backfill
r	=	Radius in the exclusion analysis
s	=	Dimensionless parameter related to the degree of capillarity of the backfill
x, y	=	vector of points for regression analysis
w_c	=	Length of the crevice or aperture (m)
z	=	elevation
z_1	=	Elevation on the inside of the drip shield
z_0	=	Elevation on the outside of the drip shield

Upper Case Arabic Variables

A_{ij}	=	Cross sectional area of the flow in branch ij
B	=	Aperture thickness
B_j	=	Aperture thickness of jth aperture size
C_p	=	Volumetric heat capacity of the tuff rock or crushed tuff rock (J/kg-K)
C_s	=	Specific heat capacity of the tuff rock or crushed tuff rock (J/kg/K)
G_s	=	Specific gravity of solids
K_0	=	Hydraulic conductivity at reference moisture potential
K_c	=	Saturated hydraulic conductivity of the combined material (cm/sec)
K_i	=	Thermal conductivity (W/m-°K)
K_s	=	Saturated hydraulic conductivity (cm/sec)
K_u	=	Unsaturated hydraulic conductivity (cm/sec)
L_c	=	Flow path length of capillary tubes through the drip shield
L_i	=	Flow path of component i
L_{DS}	=	Length of drip shield
M	=	Number of different capillary tube sizes
M_w	=	Molecular weight of water (g/mole)
N_j	=	Number of capillary tubes of radius R_j or parallel plates of width B_j
P	=	wetted perimeter
P_v	=	Water vapor pressure
P_{vsat}	=	Saturated water vapor pressure
Q	=	in-drift seepage rate
Q_{ij}	=	Branch flow rates from node i to node j in the network resistance model
Q_j	=	Flow rate through the jth capillary size tube or parallel plates
Q_T	=	Total flow rate through all capillary size tubes or parallel plates
R_j	=	Radius of the jth capillary size tube
T	=	Absolute temperature
V_s	=	Solids volume (cm ³)
V_t	=	Total volume (cm ³)
V_v	=	Void volume (cm ³)
W_s	=	Weight of solids (g)

Lower Case Greek Variables

α	=	van Genuchten or exponential curve-fitting parameters (cm ⁻¹)
θ	=	Volumetric moisture content
θ_i	=	Volumetric moisture content for the ith component of a soil
θ_r	=	Residual volumetric moisture content
θ_s	=	Saturated volumetric moisture content
ρ	=	Dry bulk mass density (g/cm ³)
ρ_r	=	Dry bulk mass density for the rock (g/cm ³)
ρ_w	=	Bulk mass density of water (g/cm ³)
σ	=	Surface tension of water on the drip shield
ν	=	Dynamic viscosity of water
ϕ	=	Porosity

ϕ_b	=	Backfill porosity
ϕ_i	=	Volumetric proportion for the ith component of a soil
ψ	=	Moisture potential (cm)
ψ_0	=	Reference moisture potential for the backfill (cm)
ψ_{ei}	=	Moisture potential for the ith component of the soil (cm)
ψ_i	=	Moisture potential inside the drip shield (cm)
ψ_j	=	Moisture potential of the jth capillary tube of radius R_j or of the jth crevice of width B_j (cm)
ψ_{jT}	=	Moisture potential of the jTth capillary tube of radius R_j or of the jth crevice of width B_j , in (cm), for which $\psi_{jT-1} < \psi_0 < \psi_{jT}$
ψ_o	=	Moisture potential outside the drip shield (cm)

Upper Case Greek Variables

ΔH	=	Difference in hydraulic potential between the inner and outer surfaces of drip shields (m)
I	=	Ratio of Kirchhoff potential Θ at some point to the reference Θ_0
Δt	=	Thickness of the drip shield
Θ	=	Kirchoff potential
Θ_0	=	Kirchoff potential at the reference moisture potential ψ_0
Θ_1	=	Kirchoff potential for saturated conditions or $\psi = 0$

Special Symbols

:=	=	Assignment statement in Mathcad 8
=	=	Output statement in Mathcad 8
•	=	Multiplication Symbol
◦	=	Multiplication symbol (only when used at centerline of text in equation)
...	=	Continuation symbol in MathCad 8

ATTACHMENT IV
MOISTURE RETENTION CHARACTERISTICS OF THE BACKFILL AND INVERT
MATERIALS

IV.1 MOISTURE RETENTION CHARACTERISTICS OF THE BACKFILL MATERIALS

This attachment describes the MathCad software routine for curve fitting and generating plots presented in the main text (Sections 6.2.1 to 6.2.4). Inputs to the MathCad routines included the absolute values of the moisture potential (ψ) in bars and volumetric moisture content (θ) measurements for the Overton Sand backfill (Section 4.1.5) from the UFA measurements. Input values are listed below. Note that in the centrifuge measurements (CRWMS M&O 1996, p. C-4), the rate of rotation is set that sets the moisture potential in the samples:

	[0.04		[0.268		[0.04		[0.169
		0.17			0.083			0.17			0.084
		0.30			0.053			0.30			0.059
		0.46			0.045			0.46			0.047
		0.67			0.036			0.67			0.036
		1.05			0.028			1.05			0.029
		1.51			0.023			1.51			0.024
		2.05			0.02			2.05			0.02
HUFA1 :=		2.90	TUFA1 :=		0.018	HUFA2 :=		2.90	TUFA2 :=		0.018
		4.18			0.016			4.18			0.015
		5.69			0.014			5.69			0.014
		7.43			0.014			7.43			0.014
		11.62			0.012			11.62			0.012
		16.73			0.012			16.73			0.011
		22.77			0.012			22.77			0.011
		29.74			0.011			29.74			0.01
		37.64			0.011			37.64			0.01
		46.47			0.002			46.47			0.009
]]]]

NOTE 1:

HUFA1	UFA Moisture Potential Measurements for Overton Sample No. 1
TUFA1	UFA Volumetric Moisture Content Measurements for Overton Sample No.1
HUFA2	UFA Moisture Potential Measurements for Overton Sample No.2
TUFA2	UFA Volumetric Moisture Content Measurements for Overton Sample No. 2

NOTE 2: These data are used in the EXCEL calculation (Attachment IV; p. IV-21), and the data are plotted in Figure IV-1.

Inputs to the MathCad routine included the absolute value of the moisture potential (ψ) in cm and volumetric moisture content (θ) measurements for the Overton Sand backfill (Section 4.1.5) from the Tempe Cell measurements. Input values are listed below.

HTEMP1 :=	$\begin{bmatrix} 1 \\ 11.9 \\ 23.4 \\ 49.7 \\ 101.1 \\ 201.28 \\ 399.84 \\ 500.48 \end{bmatrix}$	TTEMP1 :=	$\begin{bmatrix} 0.397 \\ 0.378 \\ 0.366 \\ 0.092 \\ 0.066 \\ 0.046 \\ 0.038 \\ 0.036 \end{bmatrix}$	HTEMP2 :=	$\begin{bmatrix} 1 \\ 11.9 \\ 23.4 \\ 49.7 \\ 101.1 \\ 201.28 \\ 399.84 \\ 500.48 \end{bmatrix}$	TTEMP2 :=	$\begin{bmatrix} 0.42 \\ 0.414 \\ 0.4 \\ 0.091 \\ 0.071 \\ 0.05 \\ 0.036 \\ 0.033 \end{bmatrix}$
-----------	--	-----------	--	-----------	--	-----------	--

NOTE 1:

HTEMP1 Tempe Cell Moisture Potential Measurements for Overton Sample No. 1
TTEMP1 Tempe Cell Moisture Content Measurements for Overton Sample No. 1
HTEMP2 Tempe Cell Moisture Potential Measurements for Overton Sample No. 2
TTEMP2 Tempe Cell Moisture Content Measurements for Overton Sample No. 2

NOTE 2: These data are plotted in Figure IV-1.

Define units for analysis:

$$\text{Bar} := 100 \cdot 1000 \text{ Pa}$$

$$\text{Bar} = 14.504 \text{ psi}$$

In accordance with AP-SI.Q, hand calculations listed below are used to verify the EXCEL spreadsheet calculations (Attachment IV, p. IV-21). Equation (8) (Section 6.2.1.3) is used with the results from van Genuchten curve fitting to predict the volumetric moisture content from the absolute value of moisture potential expressed in bars (Attachment IV, p. IV-21):

$$\theta_r := 0.01$$

$$\theta_s := 0.41$$

$$\alpha_b := 30.238 \text{ Bar}^{-1}$$

$$n_b := 1.986$$

For the first point, calculate the predicted moisture content:

$$\psi := .04 \text{ Bar}$$

$$\left[1 + (\alpha \cdot \psi)^n \right]^{-\left(1 - \frac{1}{n}\right)} \cdot (\theta_s - \theta_r) + \theta_r = 0.2663$$

This answer agrees with the calculation in the EXCEL spreadsheet and cell formula is verified. Calculate the square of the residual for the first point:

$$(0.2682 - 26.6325210^{-2})^2 = 3.515 \cdot 10^{-6}$$

This first residual agrees with the calculation in the EXCEL spreadsheet and cell formula is verified.

The van Genuchten parameters shown below are results from the EXCEL calculations presented in Table IV-1 (Attachment IV p. IV-21) which was developed using the first Overton sand sample:

$$\theta_r := 0.01$$

$$\theta_s := 0.41$$

$$\alpha_b := 0.03 \text{ cm}^{-1}$$

$$n_b := 1.986$$

Define the moisture retention for function from Equation (8):

$$\Theta(\alpha, n, \theta_s, \theta_r, \psi) := \left[1 + (\alpha \cdot \psi)^n \right]^{-\left(1 - \frac{1}{n}\right)} \cdot (\theta_s - \theta_r) + \theta_r$$

Note that the first sample was analyzed for curvefitting because the two samples of Overton Sand produced identical results over the range of interest. As a test case verify by hand the function presented above by substituting in the constants for an absolute value of moisture potential of 10 cm:

$$\left[1 + (0.030 \text{ cm}^{-1} \cdot 10 \cdot \text{cm})^{1.986} \right]^{-\left(1 + \frac{1}{1.986}\right)} \cdot (0.41 - 0.01) + 0.01 = 0.393$$

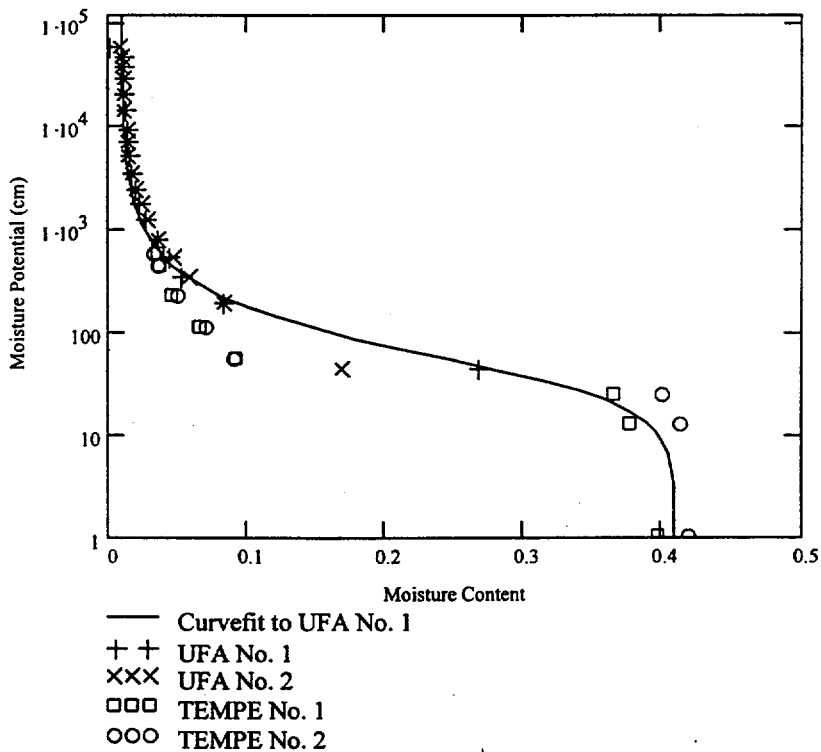
$$\Theta(\alpha, n, \theta_s, \theta_r, 10 \cdot \text{cm}) = 0.393$$

The results of the hand calculation and function are in agreement and the function is verified.

Figure IV-1 plots the data against the curvefit parameters. Define a log variable for purposes of plotting:

$$\text{logh} := 0, 0.1, .5$$

$$h(\text{logh}) := 10^{\text{logh}} \cdot \text{cm}$$



Note: Graph is based upon data presented on p. IV-2 to IV-3 with moisture potential for the UFA measurements converted to cm.

Figure IV-1. Moisture Retention Relationship for Overton Sand

IV.2 RELATIONSHIP OF UNSATURATED HYDRAULIC CONDUCTIVITY TO MOISTURE POTENTIAL AND VOLUMETRIC MOISTURE CONTENT FOR OVERTON SAND

Define the unsaturated hydraulic conductivity relation from Equation (10):

$$K(\alpha, n, \psi, K_s) := K_s \frac{\left[1 - (\alpha \cdot \psi)^{(n-1)} \cdot \left[1 + (\alpha \cdot \psi)^n \right]^{\left(-1 + \frac{1}{n} \right)} \right]^2}{\left[\left[1 + (\alpha \cdot \psi)^n \right]^{\left[\frac{1}{2} - \frac{1}{(2 \cdot n)} \right]} \right]}$$

A value for saturated hydraulic conductivity was assigned for replication 1 of Overton Sand. As shown subsequently in Figure IV-2, the value of K_s is determined by extrapolating the unsaturated hydraulic conductivity to a saturated volumetric moisture content (θ_s) of 0.41 resulting in:

$$K_s := 0.014 \frac{\text{cm}}{\text{sec}}$$

The extrapolated value is reasonable for this type of sand and agrees with a value for sand of this gradation (Freeze and Cherry 1979, p. 29). The formula presented above was verified by hand calculation (shown below) for an absolute value of moisture potential $\psi = 10$ cm and restated for other parameters (Table IV-1):

$$\psi := 10 \text{ cm}$$

$$\alpha_b := 0.03 \text{ cm}^{-1}$$

$$n_b := 1.986$$

$$K_s = 0.014 \frac{\text{cm}}{\text{sec}}$$

$$0.014 \frac{\left[1 - (0.03 \cdot 10)^{(1.986-1)} \cdot \left[1 + (0.03 \cdot 10)^{1.986} \right]^{\left(-1 + \frac{1}{1.986} \right)} \right]^2}{\left[\left[1 + (0.03 \cdot 10)^{1.986} \right]^{\left[\frac{1}{2} - \frac{1}{(2 \cdot 1.986)} \right]} \right]} = 6.864 \cdot 10^{-3}$$

$$K(\alpha, n, \psi, K_s) = 6.864 \cdot 10^{-3} \frac{\text{cm}}{\text{sec}}$$

The results of the hand calculation and the function are in agreement and the function is verified.

The measurements of unsaturated hydraulic conductivity were input as a function of volumetric moisture content (θ) for the first and second replication Overton Sand Samples (Section 4.1.5). Note that the hydraulic conductivity data were input in cm/s.

OV11:=	$0.3699 \quad 6.1 \cdot 10^{-3}$		$0.342 \quad 3.70 \cdot 10^{-3}$
	$0.3351 \quad 4.63 \cdot 10^{-4}$		$0.323 \quad 3.76 \cdot 10^{-4}$
	$0.1861 \quad 5.00 \cdot 10^{-5}$		$0.192 \quad 5.00 \cdot 10^{-5}$
	$0.107 \quad 1.8 \cdot 10^{-5}$		$0.129 \quad 1.80 \cdot 10^{-5}$
	$0.084 \quad 7.99 \cdot 10^{-6}$		$0.074 \quad 7.99 \cdot 10^{-6}$
	$0.083 \quad 3.60 \cdot 10^{-6}$		$0.065 \quad 3.60 \cdot 10^{-6}$
	$0.0715 \quad 1.35 \cdot 10^{-6}$		$0.058 \quad 1.35 \cdot 10^{-6}$
	$0.0621 \quad 4.50 \cdot 10^{-7}$		$0.048 \quad 4.50 \cdot 10^{-7}$
	$0.0559 \quad 8.99 \cdot 10^{-8}$		$0.038 \quad 8.99 \cdot 10^{-8}$
	$0.0415 \quad 3.40 \cdot 10^{-8}$		$0.034 \quad 3.40 \cdot 10^{-8}$
	$0.0357 \quad 5.76 \cdot 10^{-9}$		$0.027 \quad 5.76 \cdot 10^{-9}$
	$0.017 \quad 3.16 \cdot 10^{-10}$		$0.015 \quad 3.16 \cdot 10^{-10}$

Note that:

OV11 UFA Conductivity Measurements for Overton Sand Replication No. 1
 OV12 UFA Conductivity Measurements for Overton Sand Replication No. 2

The number of measurements in the sample were determined as:

$$\text{rows}(\text{OV11}) = 12$$

$$\text{rows}(\text{OV21}) = 12$$

Figure IV-2 plots the unsaturated hydraulic conductivity against the measurements for volumetric moisture content using Equation (8).

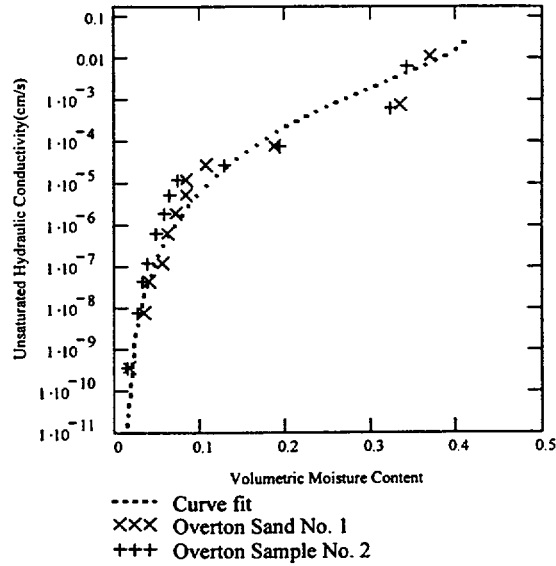


Figure IV-2. Relationship of Volumetric Moisture Content to Unsaturated Hydraulic Conductivity Backfill

Figure IV-3 plots the unsaturated hydraulic conductivity against the moisture potential (ψ) for Overton Sand using Equation (8) and the curve-fit parameters for Overton Sand Sample No.1.

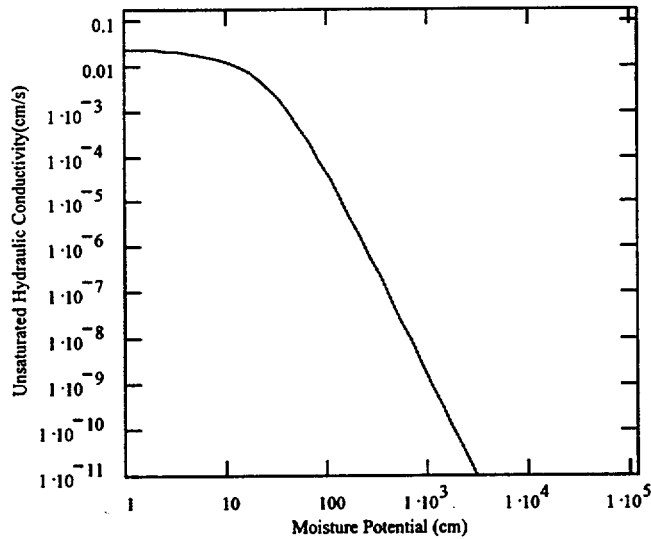


Figure IV-3. Unsaturated Hydraulic Conductivity versus Moisture Potential for Overton Sand Sample No.1

IV.3 EXPONENTIAL CURVEFIT TO MOISTURE RETENTION FOR OVERTON SAND

For each moisture retention measurement for the first replication Overton Sand sample, solve for the absolute value of moisture potential (ψ) from Equation (8) for a range of moisture potentials from zero to -440 cm for curve fitting to the exponential function (Equation (35)). A percolation rate of 25 mm per year (Assumption 5.13) corresponds to approximately 8×10^{-8} cm/sec. For the moisture potential of approximately -360 cm, the saturation level would increase resulting in a lower absolute value of moisture potential above the drip shield as discussed further in Attachment VI, p. VI-4:

$$\theta = \left[1 + (\alpha \cdot \psi)^n \right]^{-\left(1 - \frac{1}{n}\right)} \cdot (\theta_s - \theta_r) + \theta_r$$

From Equation (8), solve for the absolute value of the moisture potential in terms of the volumetric moisture content:

$$\psi = \frac{\left[-1 + \left[\frac{-(\theta - \theta_r)}{(-\theta_s + \theta_r)} \right]^{\left[\frac{-1}{(n-1)} \right]^n} \right]^{\left(\frac{1}{n} \right)}}{\alpha}$$

$i := 0..7$

Solve for the absolute value of moisture potential over the range of volumetric moisture content from the unsaturated hydraulic conductivity data for the first Overton sample:

$$\Psi_Potential_i := \frac{\left[-1 + \left[\frac{-(OV11_{i,0} - \theta_r)}{(-\theta_s + \theta_r)} \right]^{\left[\frac{-1}{(n-1)} \right]^n} \right]^{\left(\frac{1}{n} \right)}}{\alpha}$$

Define a vector for the unsaturated hydraulic conductivity over the range volumetric contents corresponding to the range of the absolute value of moisture potential from 0 to 437 cm:

$$K_Overton_1_i := OV11_{i,1}$$

Transform the unsaturated hydraulic conductivity measurements to the log plane:

$$\ln K_Overton_1_i := \ln(K_Overton_1_i)$$

Output the results:

$$\begin{array}{l}
 \Psi_{\text{Potential}} \\
 \text{cm}
 \end{array} = \begin{bmatrix} 16.149 \\ 23.943 \\ 68.823 \\ 136.12 \\ 181.418 \\ 184.025 \\ 220.048 \\ 261.238 \\ 297.623 \\ 437.51 \end{bmatrix}
 \quad
 \begin{array}{l}
 K_{\text{Overton}_1} \\
 \text{cm}
 \end{array} = \begin{bmatrix} 6.1 \cdot 10^{-3} \\ 4.63 \cdot 10^{-4} \\ 5 \cdot 10^{-5} \\ 1.8 \cdot 10^{-5} \\ 7.99 \cdot 10^{-6} \\ 3.6 \cdot 10^{-6} \\ 1.35 \cdot 10^{-6} \\ 4.5 \cdot 10^{-7} \\ 8.99 \cdot 10^{-8} \\ 3.4 \cdot 10^{-8} \end{bmatrix}
 \quad
 \begin{array}{l}
 \ln K_{\text{Overton}_1} \\
 \text{cm}
 \end{array} = \begin{bmatrix} -5.099 \\ -7.678 \\ -9.903 \\ -10.925 \\ -11.737 \\ -12.535 \\ -13.515 \\ -14.614 \\ -16.225 \\ -17.197 \end{bmatrix}$$

Use the MathCad functions (MathSoft 1998 p. 199) to define the intercept and slope using linear regression analysis. Note that the value for α or the slope m is negative because the analysis is based upon the absolute value of moisture potential:

$$\begin{aligned}
 b &:= \text{intercept}(\Psi_{\text{Potential}}, \ln K_{\text{Overton}_1}) \\
 b &= -6.957 \\
 m &:= \text{slope}(\Psi_{\text{Potential}}, \ln K_{\text{Overton}_1})
 \end{aligned}$$

$$\begin{aligned}
 \alpha &:= m \\
 \alpha &= -0.027 \text{cm}^{-1} \\
 \psi_o &:= \frac{b}{\alpha} \\
 \psi_o &= 254.916 \text{cm} \\
 K_o &:= e^{m \cdot \psi_o + b} \\
 K_o &= 9.062 \cdot 10^{-7}
 \end{aligned}$$

Define the exponential function plotting against the data (Equation 36):

$$K(\psi) := K_o \cdot e^{\alpha \cdot (\psi - \psi_o)}$$

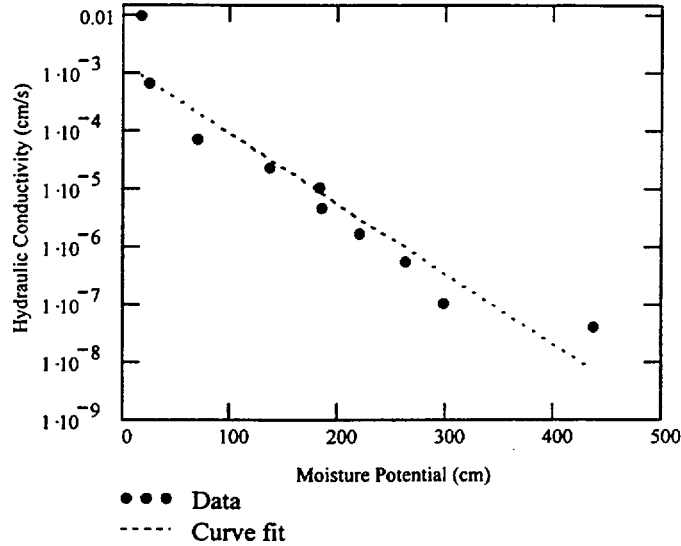


Figure V-4. Relationship of Hydraulic Conductivity to Moisture Potential Using the Exponential Relationship for Overton Sand

IV.4 MOISTURE RETENTION OF CRUSHED TUFF

Inputs to the MathCad routine included the absolute value of the moisture potential (ψ) in bars and moisture retention (θ) measurements for the crushed tuff invert (Section 4.1.5). Input values are listed below. Note again that the absolute value of moisture potential is set by the centrifuge centrifugal force per unit area per unit weight, and the volumetric moisture content is measured:

HCTU1 :=	0.121 0.174 0.309 0.483 0.696 1.090 1.93 3.02 4.35 17.4	·Bar	TCTU1 :=	0.068 0.059 0.058 0.057 0.056 0.055 0.053 0.052 0.050 0.045	HCTU2 :=	0.121 0.174 0.309 0.483 0.696 1.09 1.93 3.02 4.35 17.40	·Bar	TCTU2 :=	0.060 0.060 0.059 0.058 0.058 0.056 0.054 0.054 0.052 0.047
----------	--	------	----------	--	----------	--	------	----------	--

Note 1:

- HCTU1 UFA Moisture Potential Measurements for Crushed Tuff Sample No. 1
- TCTU1 UFA Moisture Content Measurements for Crushed Tuff Sample No. 1
- HCTU2 UFA Moisture Potential Measurements for Crushed Tuff Sample No. 2
- TCTU2 UFA Moisture Content Measurements for Crushed Tuff Sample No. 2

Note 2: These data are used in the EXCEL calculation (Attachment IV, p. IV-22) and are plotted in Figure IV-5.

Calculate the number of points for the sample:

$$\text{rows(HCTU1)} = 10$$

$$\text{rows(TCTU1)} = 10$$

$$\text{rows(HCTU2)} = 10$$

$$\text{rows(TCTU2)} = 10$$

$$i := 0..9$$

Convert the absolute value of the moisture potential from bars to cm:

$$\text{HHCTU1}_i := \frac{\text{HCTU1}_i}{62.4 \frac{\text{lb}_f}{\text{ft}^3}}$$

$$\text{HHCTU2}_i := \frac{\text{HCTU2}_i}{62.4 \frac{\text{lb}_f}{\text{ft}^3}}$$

The MathCad output resulting from the conversion of moisture potential in bars on the previous page to cm is shown below. These conversion data are plotted in Figure IV-5.

$$\text{HHCTU1} = \begin{bmatrix} 123.441 \\ 177.51 \\ 315.233 \\ 492.744 \\ 710.041 \\ 1.112 \cdot 10^3 \\ 1.969 \cdot 10^3 \\ 3.081 \cdot 10^3 \\ 4.438 \cdot 10^3 \\ 1.775 \cdot 10^4 \end{bmatrix} \text{ cm} \quad \text{HHCTU2} = \begin{bmatrix} 123.441 \\ 177.51 \\ 315.233 \\ 492.744 \\ 710.041 \\ 1.112 \cdot 10^3 \\ 1.969 \cdot 10^3 \\ 3.081 \cdot 10^3 \\ 4.438 \cdot 10^3 \\ 1.775 \cdot 10^4 \end{bmatrix} \text{ cm}$$

Note that for crushed tuff, only UFA retention measurements were performed. Note also that the samples were tested in the loose state with a dry bulk density of 0.93 g/cm^3 (Section 4.1.5). Solve for the porosity equal to θ_s using Equation (11):

$$\rho = G_s \frac{V_s}{(V_s + V_v)}$$

Substituting the values for G_s , ρ , and V_s :

$$0.93 \frac{\text{cm}}{\text{gm}^3} = \frac{2.54 \frac{\text{gm}}{\text{cm}^3}}{(1.0 \text{ cm}^3 + V_v)}$$

Solving for V_v :

$$V_v := \left(\frac{2.54}{0.93} - 1.0 \right) \cdot \text{cm}^3$$

$$V_v = 1.731 \cdot \text{cm}^3$$

Solve for the porosity (ϕ) which equals θ_s :

$$\phi := \frac{V_v}{1.0 \text{ cm}^3 + V_v}$$

$$\phi = 0.63$$

The van Genuchten parameters shown below are results from the EXCEL calculations presented in Table IV-3 (Attachment IV, p. IV-22) which was developed using the crushed tuff sieved from 2 to 4.75 mm (Section 4.1.5):

$$\theta_r := 0.05$$

$$\theta_s := 0.63$$

$$\alpha_i := 0.12$$

$$n_i := 2.75$$

Define the moisture retention for function from Equation (8) using the absolute value for moisture potential:

$$\theta(\alpha, n, \theta_s, \theta_r, \psi) := \left[1 + (\alpha \cdot \psi)^n \right]^{-\left(1 - \frac{1}{n}\right)} \cdot (\theta_s - \theta_r) + \theta_r$$

Figure IV-5 plots the data against the curve fit parameters. Define a log variable for purposes of plotting.

$$\log h := 0, 0.1.. 6$$

$$h(\log h) := 10^{\log h} \cdot \text{cm}$$

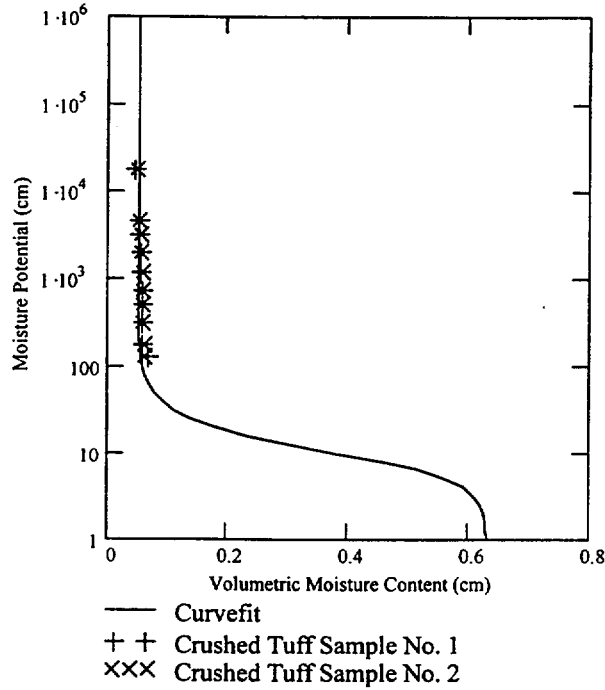


Figure IV-5. Moisture Retention Relationship for Crushed Tuff

IV.5 RELATIONSHIP OF UNSATURATED HYDRAULIC CONDUCTIVITY TO MOISTURE POTENTIAL AND VOLUMETRIC MOISTURE CONTENT FOR THE INVERT

Define the unsaturated hydraulic conductivity relation from Equation (10):

$$K(\alpha, n, \psi, K_s) := K_s \frac{\left[1 - (\alpha \cdot \psi)^{(n-1)} \cdot \left[1 + (\alpha \cdot \psi)^n \right]^{-1 + \frac{1}{n}} \right]^2}{\left[1 + (\alpha \cdot \psi)^n \right]^{\left[\frac{1}{2} - \frac{1}{(2n)} \right]}}$$

Input the saturated hydraulic conductivity for the Crushed Tuff. The value is taken from the RETC analysis (Attachment IV, p. IV-26) of the crushed tuff sample:

$$K_s := 0.60316 \frac{\text{cm}}{\text{sec}}$$

Input the measurements of unsaturated hydraulic conductivity (m/sec) as a function of volumetric moisture content (θ) for the crushed tuff sieved from 2.00 to 4.75 mm (Section 4.1.5). Note that the second sample provided identical results:

$$CS2475 := \begin{bmatrix} 0.109 & 4.28 \cdot 10^{-7} \\ 0.092 & 4.28 \cdot 10^{-8} \\ 0.076 & 1.07 \cdot 10^{-8} \\ 0.066 & 1.19 \cdot 10^{-9} \end{bmatrix}$$

Figure IV-6 plots the unsaturated hydraulic conductivity against the measurements for volumetric moisture content using Equation (9) and the curve fit parameters.

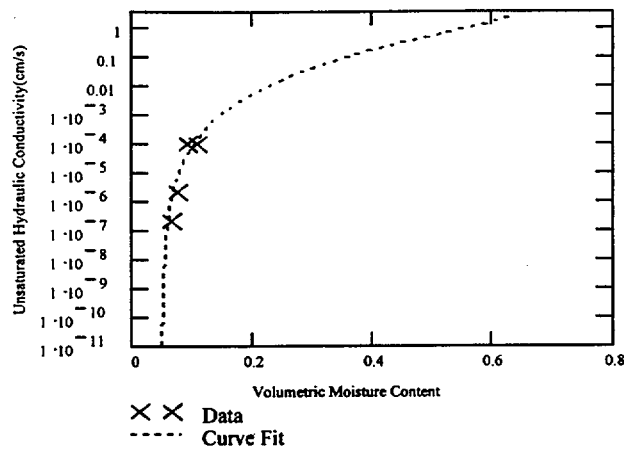


Figure IV-6. Relationship of Volumetric Moisture Content to Unsaturated Hydraulic Conductivity for Crushed Tuff

Figure IV-7 plots the unsaturated hydraulic conductivity against the volumetric moisture potential (ψ) from Equation (10) using the van Genuchten parameters for crushed tuff sieved from 2 to 4.75mm.

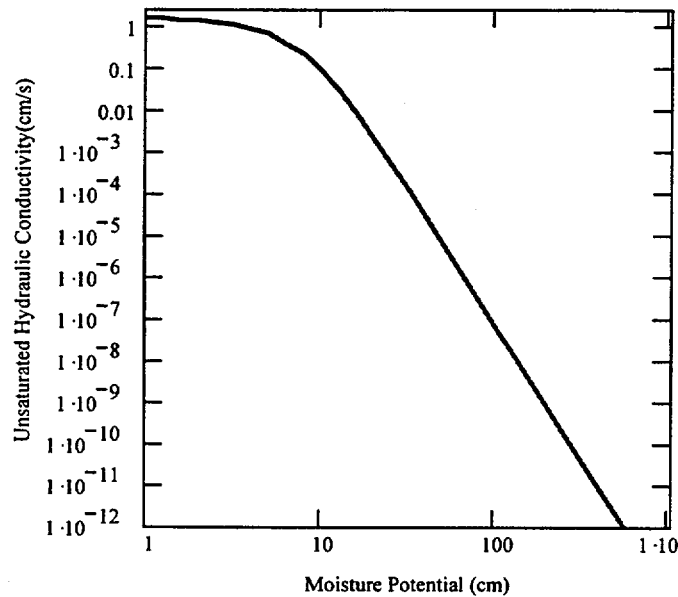


Figure IV-7. Unsaturated Hydraulic Conductivity versus Volumetric Moisture Content for Crushed Tuff Sieved from 2 to 4.75mm

IV.6 RETENTION CHARACTERISTICS FOR THE COMBINED MATERIAL

This section takes the retention relationship for the backfill and invert materials from previous sections and develops a retention relationship for a combined material. After the relationship of moisture potential to volumetric moisture content is determined for each material, the van Genuchten parameters are determined as the results from EXCEL calculations in Table IV-5 (Attachment IV-5, p. IV-23).

The van Genuchten parameters shown below are results from EXCEL calculations presented in Table IV-1 (Attachment IV, p. IV 21):

$$\theta_r := 0.01$$

$$\theta_s := 0.41$$

$$\alpha_b := 0.03$$

$$n_b := 1.986$$

Define a function for the backfill from Equation (8):

$$\Theta_{\text{backfil}}(\psi) := \left[1 + (|\alpha \cdot \psi|)^n \right]^{-\left(1 - \frac{1}{n}\right)} \cdot (\theta_s - \theta_r) + \theta_r$$

The van Genuchten parameters shown below are results from EXCEL calculations presented in Table IV-3 (Attachment IV, p. IV-22):

$$\theta_r := 0.05$$

$$\theta_s := 0.63$$

$$\alpha_i := 0.12 \text{ cm}^{-1}$$

$$n_i := 2.75$$

Define a function for the invert from Equation from Equation (8):

$$\Theta_{\text{invert}}(\psi) := \left[1 + (|\alpha \cdot \psi|)^n \right]^{-\left(1 - \frac{1}{n}\right)} \cdot (\theta_s - \theta_r) + \theta_r$$

Define a log variable for developing a log plot:

$$\text{logh} := 0, 0.1, \dots, 6$$

$$h(\text{logh}) := 10^{\text{logh}} \cdot \text{cm}$$

Develop a function that performs averaging of the two retention curves (Equation (16)) through the use of Assumption 5.9:

$$\Theta_c(\psi) := 0.5 \cdot \Theta_{\text{backfil}}(\psi) + 0.5 \cdot \Theta_{\text{invert}}(\psi)$$

Plot the retention curves in Figure IV-8 for comparison purposes.

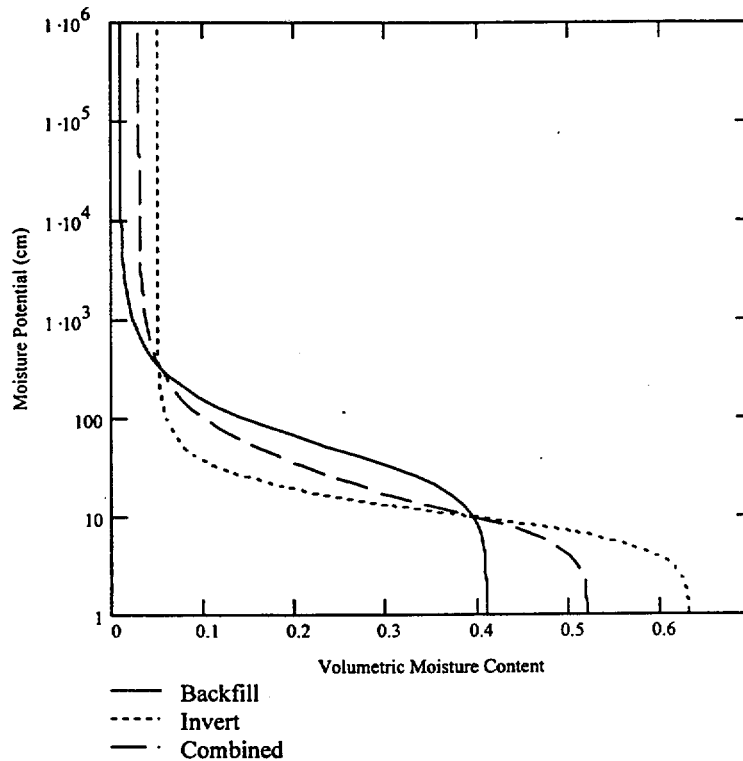


Figure IV-8. Comparison of Retention Curves for the Backfill and Invert Materials

Prepare output to perform curve fitting using Microsoft EXCEL Equation Solver as shown in Table IV-6 (Attachment IV, p. IV-23):

$$i := 1..100$$

$$\text{logh}_i := 0 + (i - 1) \cdot \frac{(5 - 1)}{100}$$

$$\theta_i := \theta_c(h(\text{logh}_i))$$

$$\text{bar} := 10^5 \cdot \text{Pa}$$

$$A_{i,0} := \theta_i$$

$$A_{i,1} := \frac{h(\text{logh}_i) \cdot 62.4 \frac{\text{lbf}}{\text{ft}^3}}{\text{bar}}$$

WRITEPRN "output") := A

Calculate the harmonic mean from Equation (18) and weighing the path length equally:

$$K_c := \frac{0.5 + 0.5 \frac{\text{cm}}{\text{sec}}}{\frac{0.5}{0.014} + \frac{0.5}{0.60316}}$$

$$K_c = 0.0274 \frac{\text{cm}}{\text{sec}}$$

Define the unsaturated flow conductivity relationship based upon the van Genuchten parameters using the absolute value for moisture potential (Ψ). From Equation (10):

$$K(\alpha, n, \psi, K_s) := K_s \frac{\left[1 - (\alpha \cdot \psi)^{(n-1)} \cdot \left[1 + (\alpha \cdot \psi)^n \right]^{-1 + \frac{1}{n}} \right]^2}{\left[1 + (\alpha \cdot \psi)^n \right] \left[\frac{1}{2} - \frac{1}{(2 \cdot n)} \right]}$$

Define a log variable for purposes of plotting.

$$h(\text{logh}) := 10^{\text{logh}} \cdot \text{cm}$$

$$\text{logh} := 0, 0.1, \dots, 4$$

Input the properties from the curve fitting analysis (Attachment IV p. IV-23)

$$\alpha_b := 0.104 \text{cm}^{-1}$$

$$n_b := 1.85$$

Plot the relationship of the unsaturated hydraulic conductivity to the moisture potential using the above equation in Figure IV-9.

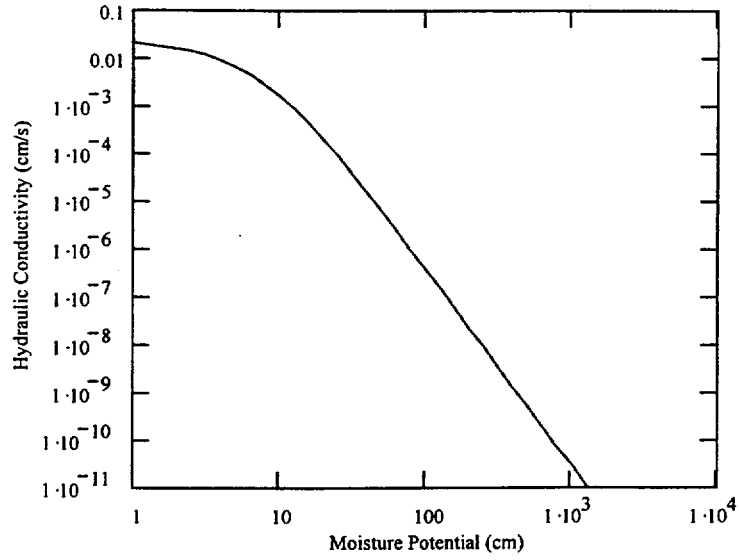


Figure IV-9. Relationship of Unsaturated Hydraulic Conductivity to Moisture Potential for the Combined Material

Table IV-1 van Genuchten Curve Fit Parameter Results for the Backfill

Moisture Content at Saturation (θ_s)	0.41		
Residual Moisture Content (θ_r)	0.01		
α_b	30.238 bars ⁻¹	0.03	cm ⁻¹
n_b	1.986		
m	0.497		
Sum of Residuals	2.13E-04		

Note that the parameters are calculated using the EXCEL Equation Solver (Section 3. P. 7 of 48) based upon the sum of the residuals as given above from Table IV-2.

Table IV-2 Retention Analysis Results for the Backfill

Volumetric Moisture Content	Moisture Potential (bars)				Predicted Moisture Content	Residuals
0.268	0.04				0.266	3.51E-06
0.083	0.17				0.089	3.50E-05
0.053	0.3				0.056	1.09E-05
0.045	0.46				0.041	1.91E-05
0.036	0.67				0.032	1.78E-05
0.028	1.05				0.024	1.12E-05
0.023	1.51				0.020	7.85E-06
0.020	2.05				0.018	4.39E-06
0.018	2.9				0.016	1.86E-06
0.016	4.18				0.015	8.60E-07
0.014	5.69				0.014	3.73E-07
0.014	7.43				0.013	2.36E-07
0.013	11.62				0.013	1.11E-09
0.012	16.73				0.012	1.31E-07
0.012	22.77				0.012	1.92E-07
0.011	29.74				0.012	6.26E-07
0.011	37.64				0.012	7.93E-07
0.002	46.47				0.012	9.84E-05

Note: Volumetric moisture content and moisture potential are obtained from Section 4.1.5 for backfill

Equation (8) is used for calculating the predicted moisture content.

Residuals are calculated as the square of the difference between the actual volumetric moisture content and the predicted moisture content.

Table IV-3 van Genuchten Curve Fit Parameter Results for the Invert

Moisture Content at Saturation (θ_s)	0.63		
Residual Moisture Content (θ_r)	0.05		
α	117.00 bars ⁻¹	0.12	cm ⁻¹
n	2.75		
m	0.64		
Sum of Residuals	5.25E-04		

Note that the parameters are calculated using the EXCEL Equation Solver (Section 3. P. 7 of 48) based upon the sum of the residuals as given above from Table IV-4.

Table IV-4 Retention Analysis Results for the Invert

Volumetric Moisture Content	Moisture Potential (bars)	Predicted Moisture Content	Residuals
0.068	0.121	0.057	1.29E-04
0.059	0.174	0.054	2.52E-05
0.058	0.309	0.052	3.49E-05
0.057	0.483	0.051	3.03E-05
0.056	0.696	0.051	2.24E-05
0.055	1.090	0.051	1.51E-05
0.053	1.930	0.051	3.83E-06
0.052	3.020	0.051	9.60E-07
0.050	4.350	0.051	1.02E-06
0.045	17.400	0.051	3.60E-05
0.060	0.121	0.057	1.14E-05
0.060	0.174	0.054	3.63E-05
0.059	0.309	0.052	4.77E-05
0.058	0.483	0.051	4.23E-05
0.058	0.696	0.051	4.54E-05
0.056	1.090	0.051	2.38E-05
0.054	1.930	0.051	8.74E-06
0.054	3.020	0.051	8.88E-06
0.052	4.350	0.051	9.79E-07
0.047	17.400	0.051	1.60E-05

Note: Volumetric moisture content and moisture potential are obtained from Section 4.1.5 for Crushed Tuff Equation (8) is used for calculating the predicted moisture content.

Residuals are calculated as the square of the difference between the actual volumetric moisture content and the predicted moisture content.

Table IV-5 Van Genuchten Curve Fit Parameter Results for the Combined Material

Moisture Content at Saturation (θ_s)	0.53			
Residual Moisture Content (θ_r)	0.03			
α_b	105.71	bars ⁻¹	0.104	cm ⁻¹
n_b	1.85			
m	0.46			
Sum of the Residuals	1.70E-03			

Note that the parameters are calculated using the EXCEL Equation Solver (Section 3. P. 7 of 48)

based upon the sum of the residuals as given above from Table IV-6.

Note for Table IV-6: Volumetric Moisture Content Values are from Equation (16) Attachment IV, p. IV-17

while the moisture potential is generated by MathCad calculations (Attachment IV, p. IV-18) for a range of moisture potential from 0.0035 to 1.703 bars. Equation (8) is used for calculating the predicted moisture content.

Residuals are calculated as the square of the difference between the actual volumetric moisture content and the predicted moisture content.

Table IV-6 Retention Analysis for the Combined Material

Volumetric Moisture Content	Moisture Potential (bars)	Predicted Moisture Content	Residuals
0.520	0.0010	0.528	6.09E-05
0.520	0.0011	0.528	5.28E-05
0.520	0.0012	0.527	4.53E-05
0.520	0.0013	0.526	3.78E-05
0.520	0.0014	0.525	2.93E-05
0.519	0.0016	0.524	2.11E-05
0.519	0.0017	0.522	1.42E-05
0.518	0.0019	0.521	7.16E-06
0.517	0.0020	0.519	2.57E-06
0.516	0.0022	0.516	1.53E-07
0.515	0.0025	0.514	8.01E-07
0.513	0.0027	0.510	5.00E-06
0.511	0.0030	0.507	1.34E-05
0.508	0.0032	0.503	2.57E-05
0.504	0.0036	0.498	4.10E-05
0.500	0.0039	0.492	5.83E-05
0.495	0.0043	0.486	7.31E-05
0.488	0.0047	0.479	8.45E-05
0.480	0.0051	0.471	8.66E-05
0.471	0.0056	0.462	8.05E-05
0.460	0.0062	0.452	6.52E-05
0.448	0.0068	0.441	4.30E-05
0.434	0.0074	0.429	1.99E-05
0.419	0.0082	0.417	3.89E-06
0.402	0.0089	0.403	4.63E-07
0.385	0.0098	0.389	1.10E-05
0.368	0.0108	0.374	3.14E-05
0.351	0.0118	0.359	5.69E-05
0.334	0.0129	0.343	7.77E-05
0.318	0.0142	0.327	8.50E-05

Table IV-6 Retention Analysis for the Combined Material (Continued)

Volumetric Moisture Content	Moisture Potential (bars)	Predicted Moisture Content	Residuals
0.287	0.01703	0.295	6.95E-05
0.273	0.01868	0.280	4.84E-05
0.259	0.02048	0.265	2.83E-05
0.247	0.02246	0.250	1.15E-05
0.234	0.02462	0.236	2.12E-06
0.223	0.027	0.222	1.28E-07
0.211	0.0296	0.209	3.97E-06
0.200	0.03246	0.197	1.17E-05
0.190	0.036	0.185	1.98E-05
0.180	0.039	0.174	2.73E-05
0.170	0.043	0.164	3.20E-05
0.160	0.047	0.154	3.29E-05
0.151	0.051	0.145	3.23E-05
0.142	0.056	0.137	2.87E-05
0.134	0.062	0.129	2.45E-05
0.126	0.068	0.122	1.94E-05
0.118	0.074	0.115	1.39E-05
0.111	0.082	0.108	9.52E-06
0.105	0.089	0.102	6.20E-06
0.099	0.098	0.097	3.25E-06
0.093	0.108	0.092	1.50E-06
0.088	0.118	0.087	4.13E-07
0.083	0.129	0.083	2.88E-08
0.078	0.142	0.079	6.67E-08
0.074	0.155	0.075	3.83E-07
0.071	0.170	0.072	9.32E-07
0.067	0.187	0.068	1.48E-06
0.064	0.205	0.065	2.03E-06
0.061	0.225	0.063	2.51E-06
0.058	0.246	0.060	2.93E-06
0.056	0.270	0.058	3.23E-06
0.054	0.296	0.056	3.42E-06
0.052	0.325	0.054	3.49E-06
0.050	0.356	0.052	3.46E-06
0.048	0.390	0.050	3.36E-06
0.047	0.428	0.048	3.21E-06
0.045	0.469	0.047	3.00E-06
0.044	0.514	0.046	2.74E-06
0.043	0.564	0.044	2.46E-06
0.042	0.619	0.043	2.18E-06
0.041	0.678	0.042	1.92E-06
0.040	0.744	0.041	1.64E-06
0.039	0.815	0.040	1.38E-06
0.038	0.894	0.039	1.14E-06
0.038	0.980	0.039	9.26E-07
0.037	1.075	0.038	7.32E-07
0.036	1.178	0.037	5.62E-07
0.036	1.292	0.037	4.07E-07
0.035	1.417	0.036	2.85E-07
0.035	1.554	0.035	1.87E-07
0.035	1.703	0.035	1.13E-07
0.034	1.868	0.034	5.37E-08
0.034	2.048	0.034	2.07E-08
0.034	2.246	0.034	3.17E-09

RETC ANALYSIS FOR THE CRUSHED TUFF INVERT

```

*****
*
* ANALYSIS OF SOIL HYDRAULIC PROPERTIES
*
* 2-4.75 Crushed Tuff (Tptpmn)
*
* MUALEM-BASED RESTRICTION, M=1-1/N
* SIMULTANEOUS FIT OF RETENTION AND CONDUCTIVITY DATA
* MTYPE= 3 METHOD= 1
*
Inputs or observed data are from Section 4.1.5
for crushed tuff *
See van Genuchten et al. 1991 for definition of variables and
output
*****

```

INITIAL VALUES OF THE COEFFICIENTS

```

=====
NO      NAME      INITIAL VALUE  INDEX
1       WCR       .0300         1
2       WCS       .6320         0
3       Alpha     .5000         1
4       n         5.0000        1
5       m         .8000         0
6       l         .5000         0
7       Ksat      .0001         1

```

OBSERVED DATA

```

=====
OBS. NO.  PRESSURE HEAD  WATER CONTENT  WEIGHTING COEFFICIENT
1          177.000  .0590         1.0000
2          315.000  .0580         1.0000
3          493.000  .0570         1.0000
4          709.000  .0560         1.0000
5         1110.000  .0550         1.0000
6         1970.000  .0530         1.0000
7         3080.000  .0520         1.0000
8         4430.000  .0500         1.0000
9        17700.000  .0450         1.0000
10         123.000  .0600         1.0000
11         177.000  .0600         1.0000
12         315.000  .0590         1.0000
13         493.000  .0580         1.0000
14         709.000  .0580         1.0000
15         1110.000  .0560         1.0000
16         1970.000  .0540         1.0000
17         3080.000  .0540         1.0000
18         4430.000  .0520         1.0000

```

19	17700.000	.0470	1.0000
	WATER CONTENT	CONDUCTIVITY	WEIGHTING COEFFICIENT
20	.1090	.4280E-04	1.0000
21	.0920	.4280E-05	1.0000
22	.0760	.1070E-05	1.0000
23	.0660	.1190E-06	1.0000

WEIGHTING COEFFICIENTS

=====

W1= 1.00000 W2=***** W12=*****

NIT	SSQ	WCR	Alpha	n	Ksat
0	.05014	.0300	.5000	5.0000	.0001
1	.05014	.0300	.0983	5.0030	.0001
2	.04964	.0301	.0286	5.6822	.0002
3	.02339	.0416	.0153	5.7738	.0094
4	.00492	.0541	.0151	7.0152	.0309
5	.00231	.0560	.0160	7.4612	.0416
6	.00219	.0571	.0178	7.1658	.0467
7	.00213	.0575	.0196	6.7883	.0513
8	.00208	.0576	.0213	6.4247	.0558
9	.00204	.0576	.0228	6.0987	.0604
51	.00104	.0559	.1160	2.7445	.6032

CORRELATION MATRIX

=====

	WCR	Alpha	n	Ksat
	1	2	3	4
1	1.0000			
2	-.1460	1.0000		
3	.4623	-.8219	1.0000	
4	-.3835	.8414	-.9958	1.0000

RSQUARED FOR REGRESSION OF OBSERVED VS FITTED VALUES = .99592182

=====

NONLINEAR LEAST-SQUARES ANALYSIS: FINAL RESULTS

=====

VARIABLE	VALUE	S.E. COEFF.	T-VALUE	95% CONFIDENCE LIMITS	
				LOWER	UPPER
WCR	.05589	.00203	27.47	.0516	.0602
Alpha	.11596	.13196	.88	-.1602	.3922
n	2.74449	.70882	3.87	1.2608	4.2282
Ksat	.60316	.77320	.78	-1.0152	2.2216

OBSERVED AND FITTED DATA

=====

NO	P	LOG-P	WC-OBS	WC-FIT	WC-DEV
1	.1770E+03	2.2480	.0590	.0589	.0001
2	.3150E+03	2.4983	.0580	.0570	.0010
3	.4930E+03	2.6928	.0570	.0564	.0006
4	.7090E+03	2.8506	.0560	.0562	-.0002

5	.1110E+04	3.0453	.0550	.0560	-.0010	
6	.1970E+04	3.2945	.0530	.0559	-.0029	
7	.3080E+04	3.4886	.0520	.0559	-.0039	
8	.4430E+04	3.6464	.0500	.0559	-.0059	
9	.1770E+05	4.2480	.0450	.0559	-.0109	
10	.1230E+03	2.0899	.0600	.0615	-.0015	
11	.1770E+03	2.2480	.0600	.0589	.0011	
12	.3150E+03	2.4983	.0590	.0570	.0020	
13	.4930E+03	2.6928	.0580	.0564	.0016	
14	.7090E+03	2.8506	.0580	.0562	.0018	
15	.1110E+04	3.0453	.0560	.0560	.0000	
16	.1970E+04	3.2945	.0540	.0559	-.0019	
17	.3080E+04	3.4886	.0540	.0559	-.0019	
18	.4430E+04	3.6464	.0520	.0559	-.0039	
19	.1770E+05	4.2480	.0470	.0559	-.0089	
	WC	K-OBS	K-FIT	K-DEV	LOGK-OBS	LOGK-FIT
20	.1090	.4280E-04	.4124E-04	.1565E-05	-4.3686	-4.3847
21	.0920	.4280E-05	.1006E-04	-.5779E-05	-5.3686	-4.9974
22	.0760	.1070E-05	.1187E-05	-.1166E-06	-5.9706	-5.9257
23	.0660	.1190E-06	.9651E-07	.2249E-07	-6.9245	-7.0154

SUM OF SQUARES OF OBSERVED VERSUS FITTED VALUES

	UNWEIGHTED	WEIGHTED
RETENTION DATA	.00030	.00030
COND/DIFF DATA	.00000	.00074
ALL DATA	.00030	.00104

SOIL HYDRAULIC PROPERTIES (MTYPE = 3)

WC	P	LOGP	COND	LOGK	DIF	LOGD
.0589	.1756E+03	2.244	.1151E-08	-8.939	.3861E-04	-4.413
.0619	.1180E+03	2.072	.1441E-07	-7.841	.1625E-03	-3.789
.0679	.7926E+02	1.899	.1806E-06	-6.743	.6851E-03	-3.164
.0799	.5318E+02	1.726	.2265E-05	-5.645	.2896E-02	-2.538
.0919	.4206E+02	1.624	.9956E-05	-5.002	.6753E-02	-2.170
.1039	.3557E+02	1.551	.2850E-04	-4.545	.1235E-01	-1.908
.1159	.3120E+02	1.494	.6450E-04	-4.190	.1979E-01	-1.704
.1279	.2800E+02	1.447	.1259E-03	-3.900	.2916E-01	-1.535
.1399	.2554E+02	1.407	.2217E-03	-3.654	.4058E-01	-1.392
.1519	.2355E+02	1.372	.3622E-03	-3.441	.5416E-01	-1.266
.1639	.2191E+02	1.341	.5592E-03	-3.252	.7004E-01	-1.155
.1759	.2052E+02	1.312	.8252E-03	-3.083	.8837E-01	-1.054
.1879	.1932E+02	1.286	.1174E-02	-2.930	.1093E+00	-.961
.1999	.1827E+02	1.262	.1622E-02	-2.790	.1330E+00	-.876
.2119	.1735E+02	1.239	.2185E-02	-2.660	.1597E+00	-.797
.2239	.1651E+02	1.218	.2882E-02	-2.540	.1896E+00	-.722
.2359	.1576E+02	1.198	.3731E-02	-2.428	.2230E+00	-.652
.2479	.1507E+02	1.178	.4755E-02	-2.323	.2602E+00	-.585
.2599	.1444E+02	1.160	.5976E-02	-2.224	.3014E+00	-.521
.2719	.1386E+02	1.142	.7419E-02	-2.130	.3471E+00	-.460
.2839	.1332E+02	1.124	.9112E-02	-2.040	.3976E+00	-.401
.2959	.1281E+02	1.108	.1108E-01	-1.955	.4534E+00	-.343
.3079	.1234E+02	1.091	.1336E-01	-1.874	.5152E+00	-.288

.3199	.1189E+02	1.075	.1598E-01	-1.796	.5834E+00	-.234
.3319	.1146E+02	1.059	.1898E-01	-1.722	.6588E+00	-.181
.3439	.1105E+02	1.043	.2241E-01	-1.650	.7422E+00	-.129
.3559	.1066E+02	1.028	.2629E-01	-1.580	.8346E+00	-.079
.3680	.1029E+02	1.012	.3068E-01	-1.513	.9371E+00	-.028
.3800	.9929E+01	.997	.3564E-01	-1.448	.1051E+01	.022
.3920	.9580E+01	.981	.4121E-01	-1.385	.1178E+01	.071
.4040	.9242E+01	.966	.4747E-01	-1.324	.1320E+01	.121
.4160	.8913E+01	.950	.5447E-01	-1.264	.1479E+01	.170
.4280	.8590E+01	.934	.6231E-01	-1.205	.1658E+01	.220
.4400	.8273E+01	.918	.7105E-01	-1.148	.1860E+01	.270
.4520	.7961E+01	.901	.8081E-01	-1.093	.2090E+01	.320
.4640	.7652E+01	.884	.9169E-01	-1.038	.2354E+01	.372
.4760	.7344E+01	.866	.1038E+00	-.984	.2657E+01	.424
.4880	.7037E+01	.847	.1173E+00	-.931	.3009E+01	.478
.5000	.6728E+01	.828	.1324E+00	-.878	.3422E+01	.534
.5120	.6416E+01	.807	.1493E+00	-.826	.3914E+01	.593
.5240	.6098E+01	.785	.1681E+00	-.774	.4505E+01	.654
.5360	.5772E+01	.761	.1893E+00	-.723	.5232E+01	.719
.5480	.5433E+01	.735	.2132E+00	-.671	.6144E+01	.788
.5600	.5078E+01	.706	.2403E+00	-.619	.7324E+01	.865
.5720	.4699E+01	.672	.2713E+00	-.567	.8911E+01	.950
.5840	.4285E+01	.632	.3072E+00	-.513	.1117E+02	1.048
.5960	.3818E+01	.582	.3496E+00	-.456	.1467E+02	1.167
.6080	.3260E+01	.513	.4013E+00	-.396	.2097E+02	1.322
.6200	.2507E+01	.399	.4691E+00	-.329	.3668E+02	1.564
.6260	.1938E+01	.287	.5154E+00	-.288	.6146E+02	1.789
.6320	.0000E+00		.6032E+00	-.220		

END OF PROBLEM

=====

ATTACHMENT V
FLOW EXCLUSION ANALYSIS

The exponential parameter result from the linear regression analysis presented in Section IV.3 (Attachment IV p. IV-10) is presented below. Note that moisture potential is negative and the absolute value of α is positive:

$$\alpha := 0.027$$

Input the diameter l as twice the radius of the drip shield (Section 4.1.1)

$$l := 2 \cdot 123.1$$

$$l = 246.2$$

Calculate the ratio s from Equation (37):

$$\frac{\alpha}{2} \cdot l = 3.324$$

Define the function for calculating the dimensionless ratio I from Equation (38)

$$I(s, r, \zeta) := 1 + 4 \cdot e^{s \cdot r \cdot \cos(\zeta)} \cdot \left[\sum_{j=1}^{20} \frac{j \cdot \ln(j, s)}{Kn(j, s)} \cdot Kn(s \cdot r) \dots + \sum_{n=1}^{20} (-1)^n \cdot Kn(n, s \cdot r) \cdot \cos(n \cdot \zeta) \cdot \left(\frac{n \cdot \ln(n, s)}{Kn(n, s)} + 2.0 \cdot \sum_{j=n+1}^{20} \frac{j \cdot \ln(j, s)}{Kn(j, s)} \right) \right]$$

Define the nondimensional radius as one:

$$a := 1.0$$

Define an array of points for developing a contour plot (MathSoft 1998, p. 259):

$$\begin{aligned} i &:= 0, 1..40 \\ j &:= 0, 1..40 \\ x_i &:= i \cdot 0.05 + .01 \\ y_j &:= (j \cdot 1 + -2) - 1 \\ x_0 &= 0.01 \\ y_0 &= 2 \\ x_{40} &= 2.01 \\ y_{40} &= -2 \end{aligned}$$

Define two functions to convert the cartesian coordinates to polar coordinates (Lide and Frederikse 1997, p. A-95) for the function:

$$\begin{aligned} r(x, y) &:= (x^2 + y^2)^{.5} \\ \theta(x, y) &:= \left(\operatorname{atan}\left(\frac{y}{x}\right) - 1 + \frac{\pi}{2} \right) \cdot 1 \end{aligned}$$

Redefine the function in terms of cartesian coordinates.

$$I_c(s, x, y) := I(s, r(x, y), \theta(x, y))$$

Define an array M for purposes of preparing a contour plot.

$$M_{i,j} := \text{if} \left(r(x_i, y_j) \geq 1.0, I_c \left(\frac{\alpha}{2} \cdot 246.2, x_i, y_j \right), 0 \right)$$

$$\frac{\alpha}{2} \cdot 246.2 = 3.324$$

Note that the function for calculating the dimensionless ratio I is verified against Phillip et al. 1989 p. 22 Figure 2 for the dimensionless parameter $s = 4.0$.

Output the maximum and minimum values from the contour plot.

$$\begin{aligned} \max(M) &= 8.318 \\ \min(M) &= 0 \end{aligned}$$

Consider the percolation flux of 25 mm per year (Section 5.13). The corresponding for ψ_0 is -360 cm (Attachment IV p. IV-9).

Develop the ratio function from Equations (33) and (34)

$$\text{Ratio}(\psi) = \frac{\Theta}{\Theta_0}$$

Note that the ratio does not depend on K_0 .

$$\text{Ratio}(\psi) := \frac{\int_{-100000}^{\psi} e^{(\xi - \psi_0)^{\alpha}} d\xi}{\int_{-100000}^{\psi_0} e^{(\xi - \psi_0)^{\alpha}} d\xi}$$

Verify that the ratio is 1 for $\psi = \psi_0$

$$\text{Ratio}(\psi_0) = 1$$

Plot the results in Figure V-1.

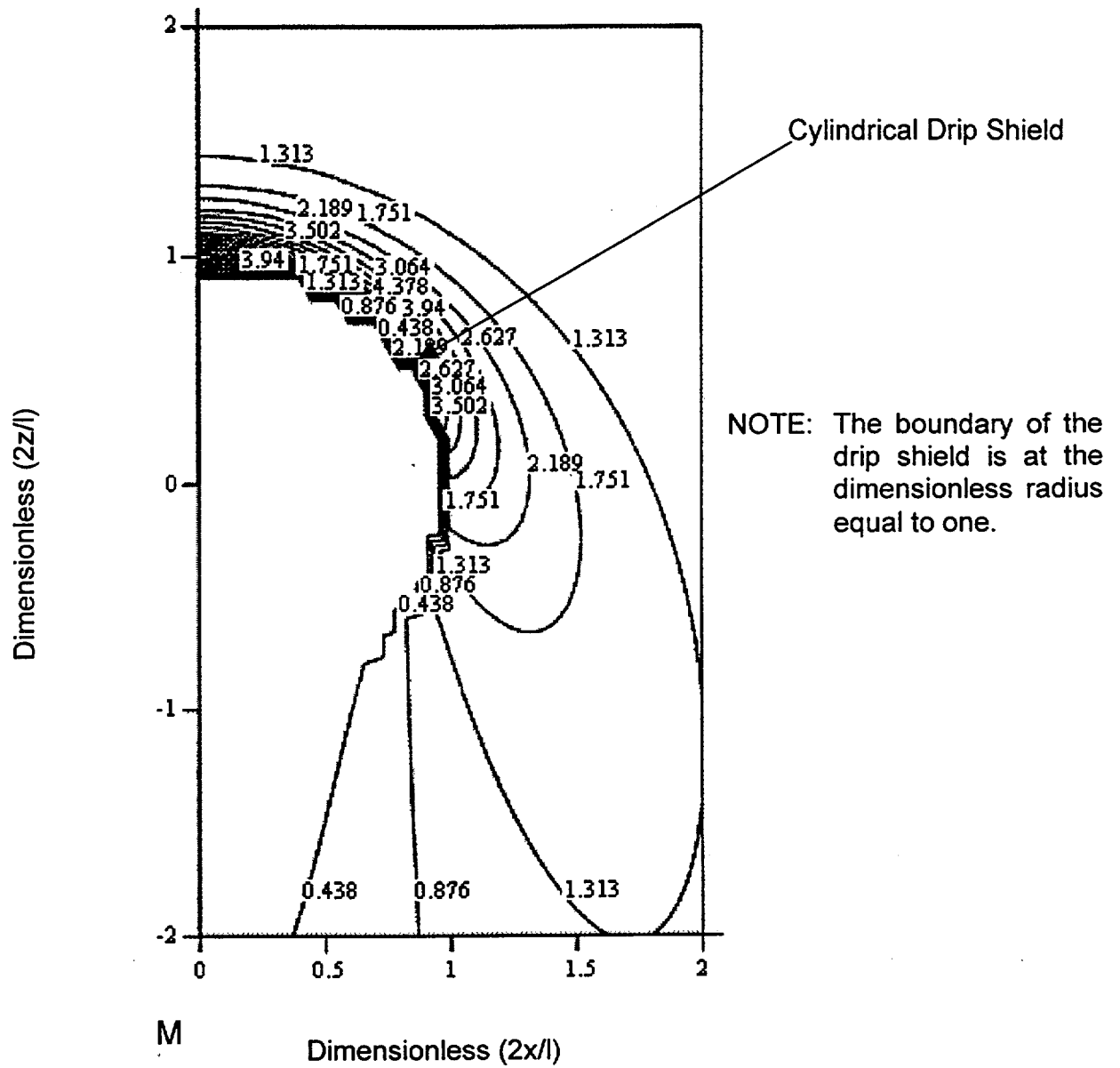


Figure V-1. Seepage About Cylindrical Drip Shield

Use MathCad Root Function (MathSoft 1998, page 187) to calculate the moisture potential corresponding to the maximum I ratio.

$$\psi := -100$$

$$\text{root}(\text{Ratio}(\psi) - 8.318, \psi) = -281.539$$

$$\text{Ratio}(-281.539) = 8.318$$

ATTACHMENT VI
BOUNDING ANALYSIS FOR A DRIP SHIELD

Input the properties of Water at 60 C (Section 4.1.2):

$$\rho_w := 0.98320 \cdot \frac{\text{gm}}{\text{cm}^3}$$

$$\nu := 466 \cdot 10^{-6} \cdot \text{Pa} \cdot \text{sec}$$

$$\sigma := 66.24 \cdot 10^{-3} \cdot \frac{\text{N}}{\text{m}}$$

Input the properties of the Drip Shield (Section 4.1.6):

$$L_c := 10 \cdot \text{cm}$$

$$L_{DS} := 5.485 \cdot \text{m}$$

Input the thickness of the drip shield (Section 4.1.6):

$$\Delta t := 2.0 \cdot \text{cm}$$

Define the function for the drip shield from Equation (42):

$$K_{DS}(\psi) := \frac{\rho_w \cdot g}{12 \cdot \nu} \cdot \frac{\Delta t}{L_c} \cdot \left(\frac{2 \cdot \sigma}{\rho_w \cdot g \cdot \psi} \cdot 1 \right)^3 \cdot \frac{1}{L_{DS}}$$

Check the calculation by hand:

$$\psi := 100 \cdot \text{cm}$$

Calculate the aperture:

$$\left(\frac{\rho_w \cdot g}{12 \cdot \nu} \right) = 1.72423 \cdot 10^6 \cdot \text{m}^{-1} \cdot \text{s}^{-1}$$

$$\left(\frac{\Delta t}{L_c} \right) = 0.2$$

$$\frac{2 \cdot \sigma}{\rho_w \cdot g \cdot \psi} = 0.01374 \cdot \text{mm}$$

$$\left(\frac{\rho_w \cdot g}{12 \cdot v}\right) \cdot \left(\frac{\Delta t}{L_c}\right) \cdot \left(\frac{2 \cdot \sigma \cdot 1}{\rho_w \cdot g \cdot \psi}\right)^3 \cdot \frac{1}{L_{DS}}$$

$$1.724 \cdot 10^6 \text{ m}^1 \cdot \text{s}^{-1} \cdot 0.20 \cdot (0.01374 \cdot \text{mm})^3 \cdot \frac{1}{5485 \cdot \text{mm}} = 1.63084 \cdot 10^{-8} \frac{\text{cm}}{\text{sec}}$$

$$K_{DS}(100 \cdot \text{cm}) = 1.63084 \cdot 10^{-8} \frac{\text{cm}}{\text{sec}}$$

The results of the hand calculation agree with the output of the function. Input the saturated hydraulic conductivity (Attachment IV, p. IV-6), and van Genuchten parameters for of the backfill (Attachment IV, p. IV-21):

$$K_s := 0.014 \frac{\text{cm}}{\text{sec}}$$

$$\alpha_b := 0.03 \text{cm}^{-1}$$

$$n_b := 1.986$$

$$K_b(\psi) := K_s \cdot \frac{\left[1 - (|\alpha \cdot \psi|)^{(n-1)} \cdot [1 + (|\alpha \cdot \psi|)^n]^{-1 + \frac{1}{n}}\right]^2}{\left[1 + (|\alpha \cdot \psi|)^n\right]^{\left[\frac{1}{2} - \frac{1}{(2 \cdot n)}\right]}}$$

Input the maximum percolation rate of 25 mm per year at the repository horizon for the present day climate (Section 5.13):

$$\psi := 300 \text{ cm}$$

$$\text{root} \left[\left[\frac{K_b(\psi)}{\frac{\text{cm}}{\text{sec}}} - 25 \cdot \frac{\frac{\text{mm}}{\text{yr}}}{\frac{\text{cm}}{\text{sec}}} \cdot 10^8, \psi \right] \right] = 363.409 \text{ cm}$$

$$\text{logh} := 1, 1.01 \dots 5$$

$$h(\text{logh}) := 10^{\text{logh}} \text{ cm}$$

Figure VI-1 presents the relationship of the equivalent conductivity to moisture potential for the drip shield for comparison to the relationship for the backfill.

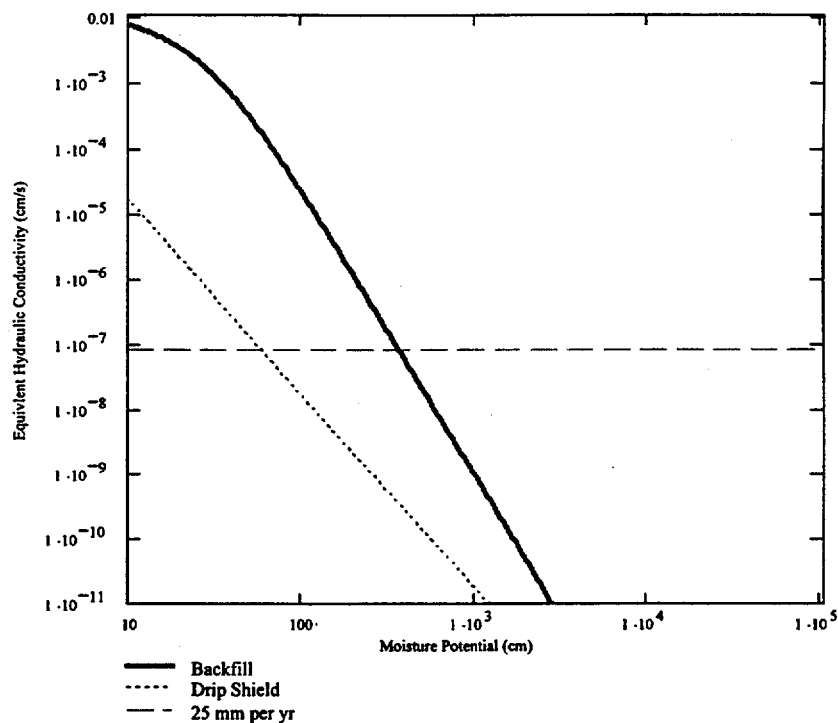


Figure VI-1. Bounding Relationship of the Equivalent Conductivity to Moisture Potential for a Drip Shield